

1 **The EMEP Intensive Measurement Period campaign,**  
2 **2008–2009: Characterizing the carbonaceous aerosol at**  
3 **nine rural sites in Europe**

4 Karl Espen Yttri<sup>\*a</sup>, David Simpson<sup>b,c</sup>, Robert Bergström<sup>c,d</sup>, Gyula Kiss<sup>e</sup>, Sönke  
5 Szidat<sup>f</sup>, Darius Ceburnis<sup>g</sup>, Sabine Eckhardt<sup>a</sup>, Christoph Hueglin<sup>h</sup>, Jacob Klenø  
6 Nøjgaard<sup>i</sup>, Cinzia Perrino<sup>j</sup>, Ignazio Pizzo<sup>a</sup>, Andre Stephan Henry Prevot<sup>k</sup>, Jean-  
7 Philippe Putaud<sup>l</sup>, Gerald Spindler<sup>m</sup>, Milan Vana<sup>n</sup>, Yan-Lin Zhang<sup>ikm</sup>, Wenche Aas<sup>a</sup>

8

9 <sup>a</sup>NILU — Norwegian Institute for Air Research (NILU), N-2027 Kjeller, Norway

10 <sup>b</sup>Norwegian Meteorological Institute, 0313 Oslo, Norway

11 <sup>c</sup>Department of Space, Earth and Environment, Chalmers University of Technology, 41296 Gothenburg

12 <sup>d</sup>Swedish Meteorological and Hydrological Institute, 60176 Norrköping, Sweden

13 <sup>e</sup>MTA-PE Air Chemistry Research Group, 8200 Veszprém – Hungary

14 <sup>f</sup>Department of Chemistry and Biochemistry & Oeschger Centre for Climate Change Research,  
15 University of Bern, 3012 Berne, Switzerland

16 <sup>g</sup>School of Physics and Centre for Climate and Air Pollution Studies, Ryan Institute, National  
17 University of Ireland Galway, Galway, Ireland

18 <sup>h</sup>EMPA, CH-8600 Duebendorf, Switzerland

19 <sup>i</sup>National Environmental Research Institute, DK-4000 Roskilde, Denmark

20 <sup>j</sup>CNR — Institute of Atmospheric Pollution Research, 00015 Monterotondo Stazione (Rome), Italy

21 <sup>k</sup>Paul Scherrer Institut, 5232 Villigen-PSI, Switzerland

22 <sup>l</sup>European Commission, Joint Research Centre, I-21027 Ispra (VA), Italy

23 <sup>m</sup>Leibniz Institute for Tropospheric Research, 04318 Leipzig, Germany

24 <sup>n</sup>The Czech Hydrometeorological Institute (CHMI), Prague, Czech Republic

25

26 <sup>\*</sup>To whom correspondence should be addressed: E-mail address: key@nilu.no

27

28 **Abstract**

29 Carbonaceous aerosol (Total Carbon;  $TC_p$ ) was source apportioned at nine European rural background  
30 sites, as part of the EMEP Intensive Measurement Periods in fall 2008 and winter/spring 2009. Five  
31 predefined fractions were apportioned based on ambient measurements: Elemental and organic carbon  
32 from combustion of biomass ( $EC_{bb}$  and  $OC_{bb}$ ) and from fossil fuel ( $EC_{ff}$  and  $OC_{ff}$ ) sources, and  
33 remaining non-fossil organic carbon ( $OC_{mf}$ ), dominated by natural sources.

34  $OC_{mf}$  made a larger contribution to  $TC_p$  than anthropogenic sources ( $EC_{bb}$ ,  $OC_{bb}$ ,  $EC_{ff}$  and  $OC_{ff}$ ) at  
35 four out of nine sites in fall, reflecting the vegetative season, whereas anthropogenic sources dominated  
36 at all but one site in winter/spring. Biomass burning ( $OC_{bb}+EC_{bb}$ ) was the major anthropogenic source  
37 at the Central European sites in fall, whereas fossil fuel ( $OC_{ff}+EC_{ff}$ ) sources dominated at the  
38 southernmost and the two northernmost sites. Residential wood burning emissions explained 30–50%  
39 of  $TC_p$  at most sites in the first week of sampling in fall, showing that this source can be dominating  
40 even outside the heating season. In winter/spring, biomass burning was the major anthropogenic source  
41 at all but two sites, reflecting increased residential wood burning emissions in the heating season.  
42 Fossil fuel sources dominated EC at all sites in fall, whereas there was a shift towards biomass burning  
43 for the southernmost sites in winter/spring.

44 Model calculations based on base-case emissions (mainly officially reported national emissions)  
45 strongly under-predicted observational derived levels of  $OC_{bb}$  and  $EC_{bb}$  outside Scandinavia. Emissions  
46 based on a consistent bottom-up inventory for residential wood burning (and including intermediate  
47 volatility compounds, IVOC), improved model results compared to the base-case emissions, but  
48 modelled levels were still substantially underestimated compared to observational derived  $OC_{bb}$  and  
49  $EC_{bb}$  levels at the southernmost sites.

50 Our study shows that natural sources is a major contributor to carbonaceous aerosol in Europe  
51 even in fall and in winter/spring, and that residential wood burning emissions are equally large or larger  
52 than that of fossil fuel sources, depending on season and region. The poorly constrained residential  
53 wood burning emissions for large parts of Europe shows the obvious need to improve emission  
54 inventories, with harmonization of emission factors between countries likely being the most important  
55 step to improve model calculations for biomass burning emissions, and European  $PM_{2.5}$  concentrations  
56 in general.

57

## 58 **Introduction**

59 Atmospheric aerosol particles play an important role in a number of environmental topics such as the  
60 radiation transfer of the Earth's atmosphere, the hydrological cycle as well as air quality, and thus have  
61 a substantial impact on the biosphere, including human health (Pope and Dockery, 2006; Andreae and  
62 Ramanathan, 2013). Carbonaceous matter is an important component of aerosol particles that has been  
63 found to account for 10–40% of PM<sub>10</sub> in the European rural background environment, 20–50% of  
64 PM<sub>2.5</sub> in urban and rural locations, and up to 70% of PM<sub>1</sub> (Zappoli et al., 1999; Putaud et al., 2010;  
65 Yttri et al., 2007a; Zhang et al., 2007; Querol et al., 2009). The carbonaceous matter is the least  
66 understood fraction of atmospheric aerosol particles due to its complexity in terms of composition,  
67 sources and formation mechanisms (Gelencsér, 2004; Pöschl, 2005; Hallquist et al., 2009; Ziemann  
68 2012). Nevertheless, it is considered to have specific impacts on global climate (Novakov and Penner,  
69 1993; Kanakidou et al., 2005), and on human health (Bell et al., 2009; Rohr and Wyzga, 2012; Cassee  
70 et al., 2013).

71 Particulate carbonaceous matter covers a wide range of organic components from low molecular  
72 weight hydrocarbons, through complex mixtures of humic-like substances and high molecular weight  
73 biopolymers containing also oxygen, nitrogen and sulphur, to tar balls or particles consisting of  
74 graphene layers. This continuum in chemical composition is reflected also in its thermochemical and  
75 optical properties (Pöschl et al., 2003). The carbonaceous fraction is usually quantified by its carbon  
76 content (total carbon, TC), which can be operationally divided into carbonate, organic carbon (OC),  
77 and elemental (EC) or black carbon (BC).

78 The complexity of carbonaceous aerosol originates from the diversity of its sources and formation  
79 processes. Carbonaceous particles are emitted both from anthropogenic (e.g. fossil fuel and biomass  
80 combustion) and biogenic sources (e.g. primary biological aerosol particles, PBAP, such as fungal  
81 spores, bacteria and degraded plant material). In addition to primary aerosol (emitted in particle form),  
82 carbonaceous aerosol can form by atmospheric oxidation of volatile precursors emitted by the  
83 vegetation or anthropogenic sources. Because of its influence on climate forcing and adverse health  
84 effects, as well as its considerable contribution to particulate mass, source apportionment of  
85 carbonaceous aerosol is of key importance. By <sup>14</sup>C-analysis, carbonaceous aerosol from fossil and  
86 modern sources can be distinguished and quantified (Szidat et al., 2004; Szidat et al., 2009; Heal et al.,  
87 2011), and whereas fossil carbon is only emitted as a consequence of human activities, modern carbon  
88 originates from both biogenic and anthropogenic sources. Thus, source-specific tracers are necessary to  
89 apportion the modern carbon content. Levoglucosan, characteristic for wood burning emission, is the  
90 most commonly used macrotracer, whereas arabitol, mannitol and cellulose are used to distinguish  
91 different types of PBAP, another source of contemporary carbon. The combination of <sup>14</sup>C and source-  
92 specific organic tracer analysis has proved to be an efficient method for source apportionment of the  
93 carbonaceous aerosol (Gelencsér et al., 2006; Gilardoni et al., 2011; Yttri et al. 2011a, b; Liu et al.,  
94 2016). Studies combining <sup>14</sup>C- and <sup>13</sup>C-analysis for source apportionment are also reported (Ceburnis et  
95 al. 2011).

96 Globally, biomass burning is the major source of the carbonaceous aerosol (Crutzen and Andreae,  
97 1990; Gelencsér, 2004), but the form and volume combusted (savanna fires, tropical forest fires,

98 agricultural waste burning, residential wood burning, etc.) depend highly on the geographical position,  
99 climate and economic situation. In Europe, wood burning for residential heating, wild fires and  
100 agricultural waste burning are the dominant forms of biomass burning, and thus significant sources of  
101 carbonaceous aerosol, although these sources were hardly recognized for large parts of Europe, until  
102 recently. Reviewing source apportionment studies of particulate matter in Europe between 1987 and  
103 2007, Viana et al. (2008) stated that in spite of its importance at certain locations, biomass combustion  
104 had rarely been identified as a substantial contributor to PM levels. Gelencsér et al. (2007) and May et  
105 al. (2009) studied anthropogenic versus natural contribution to the total organic carbon content in  
106 aerosol samples collected at six non-urban sites along a west-east transect over Europe from the Azores  
107 (Portugal) to K-puszta (Hungary) and found biogenic sources to dominate at all sites in summer. In  
108 winter most of the carbonaceous aerosol was emitted from anthropogenic sources, but there was a  
109 considerable difference in the contribution of biomass burning and fossil fuel combustion, depending  
110 on the geographical location (primarily altitude) of the sampling sites. Recently, a number of  
111 measurement based studies have discussed the role of residential wood burning as a source of air  
112 pollution in European urban and rural environments. As an example, road traffic and wood combustion  
113 contributed equally to the annual mean PM<sub>10</sub> concentrations at various sites in Switzerland (Gianini et  
114 al., 2012). In rural environment in the Alps, the contribution of wood burning to PM<sub>10</sub> even exceeded  
115 that of road traffic (Gianini et al., 2012), and in Alpine valleys wood burning was the dominant source  
116 of carbonaceous particles in wintertime (Szidat et al., 2007; Gilardoni et al., 2011; Herich et al., 2014;  
117 Zotter et al., 2014). Similar results were found both in rural and urban environments in Norway by Yttri  
118 et al. (2011a), who concluded that 80–90% of the winter time carbonaceous aerosol was emitted from  
119 anthropogenic sources, and that wood burning contributed slightly more than fossil-fuel sources. In  
120 summer, however, 70% of TC was attributed to natural sources in the rural environment, whereas the  
121 corresponding number for the urban environment was 50%.

122 Modelling studies from recent years confirm that wood burning emissions are important in  
123 wintertime Europe, and that such emissions seem to be severely underestimated in many regions  
124 (Simpson et al., 2007; Bergström et al., 2012; Genberg et al., 2013). Denier van der Gon et al. (2015a)  
125 pointed at inconsistent emission factors as a major problem (some countries report mainly solid  
126 emissions, whereas others include substantial amounts of condensed semi-volatile OC, SVOC), and  
127 produced a new bottom-up emission inventory for residential wood burning emissions of OC and EC,  
128 using a consistent methodology across Europe (see also Genberg et al., 2013). Modelling work based  
129 upon this inventory, and also including associated intermediate volatility compounds (IVOC),  
130 improved model results for both EC and OC at European regional background sites (Genberg et al.,  
131 2013 and Denier van der Gon et al., 2015a) but, so far, only limited comparisons to source  
132 apportionment data have been made with model simulations using the new inventory.

133 The EMEP (European Measurement and Evaluation Program) task force on measurement and  
134 modelling (TFMM) periodically arranges intensive measurement periods (IMPs), as a supplement to  
135 the continuous monitoring in EMEP (Aas et al., 2012). The present study is part of the second EMEP  
136 IMP, which was organized in cooperation with the EU-funded project EUCAARI (European Integrated  
137 project on Aerosol, Cloud, Climate, and Air Quality Interactions: Kulmala et al., 2009; Crippa et al.,

138 2014) in fall 2008 and winter/spring 2009. In this study, collection of aerosol filter samples and  
139 measurements of  $^{14}\text{C}$ , levoglucosan and OC/EC were harmonized by common protocol and analysis in  
140 centralized laboratories. The objective was to provide quantitative estimates of carbonaceous aerosol  
141 from fossil fuel, biomass burning and natural sources in the European rural background environment,  
142 and to study their relative contribution in two transition periods, in which a noticeable signal from all  
143 the considered sources was expected. The carbonaceous aerosol apportioned to biomass burning was  
144 used to evaluate model simulated  $\text{EC}_{\text{bb}}$  and  $\text{OC}_{\text{bb}}$  with both a base-case emission inventory, based  
145 mainly on official nationally reported emissions, and a recent, consistent, bottom-up estimate of  
146 residential combustion emissions. In the current paper we present the main findings from our study.

147

## 148 **1. Experimental**

### 149 **1.1 Site description and measurement period**

150 Aerosol filter samples were collected at nine European rural background sites (Table 1, Figure 1) for a  
151 fall period (17 September–15 October 2008; denoted Fall) and a winter/spring period (25 February–25  
152 March 2009; denoted Winter/spring). For a description of the sampling sites, see Appendix A.

153

### 154 **1.2 Aerosol sampling**

155 Ambient aerosol filter samples were obtained using various low volume filter samplers equipped with a  
156  $\text{PM}_{10}$  inlet, collecting aerosol on prefired (850 °C; 3 h) quartz fiber filters (Whatman QMA; 47 mm in  
157 diameter, batch number 11415138). The only exception was for samples collected at the Mace Head  
158 station, which used a high volume sampler with a  $\text{PM}_{2.5}$  inlet. The samplers were operated at a flow  
159 rate ranging from 16.7 l  $\text{min}^{-1}$  to 1.71  $\text{m}^3 \text{min}^{-1}$ , corresponding to a filter face velocity ranging from 20  
160 to 69  $\text{cm s}^{-1}$  (Table 1). The filter samples were collected according to the Quartz fiber filter behind  
161 Quartz fiber filter (QBQ) approach to provide a quantitative estimate of the positive sampling artefact  
162 of organic carbon (OC), thus the impact of the different filter face velocities at the various sites should  
163 be minimized. The sampling time was one week, and four samples were collected at each site for each  
164 of the two periods. At Mace Head, the collection of filter samples deviated slightly from the protocol in  
165 Fall 2008, as the second week of sampling was divided into two to separate polluted air masses passing  
166 over the European continent for the first three days of the week and clean marine air masses for the last  
167 four days of the week. The sampling inlets were installed approximately 4 m above ground level,  
168 except at Mace Head (10 m). Post exposure, filter samples were placed in petri-slides and stored in a  
169 freezer (-18 °C) to prevent degradation or evaporation of the analytes.

170

### 171 **1.3 Thermal-optical analysis**

172 Total carbon (TC), elemental carbon (EC), and organic carbon (OC) were quantified using the Sunset  
173 Lab OC-EC Aerosol Analyzer (Birch and Cary, 1996), using transmission for charring correction and  
174 operated according to the EUSAAR-2 temperature program (Cavalli et al., 2010)

175

176 **1.4 Determination of non-fossil TC from  $^{14}\text{C}$  analysis**

177 For the measurement of  $^{14}\text{C}(\text{TC}_p)$  ( $^{14}\text{C}$  of particulate TC), 0.2–2 cm<sup>2</sup> punches, corresponding to 4–40  
178  $\mu\text{g}$  TC, were transferred into preheated quartz tubes (4 mm outer diameter) filled with ~0.1 g cupric  
179 oxide. The tubes were connected to a vacuum line, cooled to -70 °C, evacuated to  $<10^{-3}$  hPa within one  
180 minute and then sealed. The sealed ampoules were heated to 850 °C for 4 hours for oxidation of TC to  
181 carbon dioxide (Fahrni et al., 2010).  $^{14}\text{C}$  measurements were performed at the Laboratory of Ion Beam  
182 Physics of ETH Zurich, using the accelerator mass spectrometer MICADAS, equipped with a gas ion  
183 source (Ruff et al., 2007), which allowed a direct injection of the carbon dioxide after dilution with  
184 helium (Wacker et al., 2013).  $^{14}\text{C}$  results for the front filters were corrected for SVOC contributions  
185 using the TC mass of the corresponding back filters and the mean  $^{14}\text{C}$  result of the four back filters for  
186 the respective site and season.  $^{14}\text{C}(\text{TC}_p)$  values are given as fractions modern ( $F^{14}\text{C}$ ), i.e. as the  $^{14}\text{C}/^{12}\text{C}$   
187 ratios of the samples related to the isotopic ratio of the reference year 1950 (Reimer et al., 2004). For  
188 determination of the non-fossil fraction of  $\text{TC}_p$  (i.e.,  $f_{\text{nf}}(\text{TC}_p)$  from  $^{14}\text{C}(\text{TC}_p)$  determinations, a reference  
189  $F^{14}\text{C}$  value of pure non-fossil emissions of  $1.08 \pm 0.04$  was used to consider the different impacts of  
190 excess  $^{14}\text{C}$  from atmospheric nuclear bomb tests to fresh biomass and tree wood (Mohn et al., 2008).  
191 This is based on the assumptions that 50% of non-fossil TC originates from fresh biomass and 50%  
192 from burning of wood, whereof the latter includes 10-year, 20-year, 40-year, 70-year and 85-year old  
193 trees with weights of 0.2, 0.2, 0.4, 0.1, and 0.1, respectively.

194

195 **1.5 Measurement of levoglucosan, mannosan and galactosan**

196 Quantification of the monosaccharide anhydrides (MA) levoglucosan, mannosan and galactosan was  
197 performed according to the method described by Dye and Yttri (2005), which has been successfully  
198 applied for aerosol samples ranging from the urban (e.g. Fuller et al., 2014) to the remote environment  
199 (e.g. Yttri et al. 2014).

200 For the analysis, punches (1.5 cm<sup>2</sup>) of the filter were spiked with  $^{13}\text{C}_6$ -levoglucosan and  $^{13}\text{C}_6$ -  
201 galactosan and extracted twice with 2 ml tetrahydrofuran under ultrasonic agitation (30 min). The  
202 filtered extracts (Teflon syringe filter, 0.45  $\mu\text{m}$ ) were evaporated to a total volume of 1 ml in a nitrogen  
203 atmosphere. Before analysis the sample solvent elution strength was adapted to the mobile phase by  
204 adding Milli-Q water (0.8 ml). The concentrations of the MAs were determined using High-  
205 Performance Liquid Chromatography (HPLC) (Agilent model 1100) in combination with HRMS-TOF  
206 (high resolution time-of-flight mass spectrometry, Micromass model LCT) operated in the negative ESI  
207 mode. Levoglucosan, mannosan and galactosan were identified on the basis of retention time and mass  
208 spectra of authentic standards. Quantification was performed using isotope labeled standards of  
209 levoglucosan and galactosan. The mass traces at  $m/z$  161.0455 and 167.0657 were used for  
210 quantification (approximately 50 mDa peak width).

211 The method described has been subject to intercomparison (Yttri et al., 2015).

212

## 213 1.6 Measurement uncertainties

### 214 1.6.1 Estimating the positive sampling artefact of OC

215 Table 2a and b show the  $OC_{Back}/OC_{Front}$  ratios for the various sites.  $OC_{Back}$  is gaseous OC present on the  
216 back filter and  $OC_{Front}$  is the sum of gaseous and particulate OC on the front filter. This ratio provides  
217 an estimate of the magnitude of the positive sampling artefact (i.e. adsorption of semi volatile organic  
218 species on the filter/ collected particles) of OC when using tandem filter sampling. When subtracting  
219  $OC_{Back}$  from  $OC_{Front}$ , positive-artefact-corrected particulate organic carbon ( $OC_p$ ) is obtained.

220 The positive artefact of OC ranged from  $5.9\pm 1.0\%$  (K-pusztá, HU) to  $28\pm 13\%$  (Lille Valby,  
221 DK) in fall, whereas the corresponding range in winter/spring was  $6.6\pm 1.3\%$  (Ispra, IT) to  $30\pm 10\%$   
222 (Lille Valby, DK). This shows that  $OC_p$  could be severely overestimated if the positive artefact was not  
223 accounted for. Note that the QBQ approach does not account for any negative artefacts (i.e. release of  
224 semi volatile organic species from collected particles), thus the  $OC_p$  levels should be considered as  
225 conservative estimates. There was typically a minor difference in the magnitude of the positive artefact  
226 between fall and winter/spring. No seasonal pattern consistent for all sites was observed.

227

### 228 1.6.2 Uncertainties in OC/EC measurements

229  $\sim 15\ \mu\text{g EC cm}^{-2}$  is considered the upper limit for the Sunset Lab OC-EC Aerosol Analyzer  
230 (Subramanian et al., 2006; Wallén et al., 2010), and should not be exceeded in order to obtain a correct  
231 OC/EC split. A non-biased OC/EC split also requires that either pyrolytic carbon (PC) evolves before  
232 EC or that PC and EC have the same light absorption coefficient, which we know is not always the case  
233 (Yang and Yu, 2002). In Fall 2008 11/36 samples exceeded  $15\ \mu\text{g EC cm}^{-2}$ , whereas the corresponding  
234 number for winter/spring 2009 was 3/36. For most of these samples the concentration just barely  
235 exceeded  $15\ \mu\text{g EC cm}^{-2}$ , nevertheless there is an added, non-quantifiable, uncertainty for these  
236 samples compared to those for which  $EC < 15\ \mu\text{g C cm}^{-2}$ .

237

### 238 1.6.3 Uncertainties in levoglucosan analysis

239 Yttri et al. (2015) reported that the analytical method used to quantify levoglucosan in the current study  
240 had a bias of  $-13\pm 4\%$  compared to the assigned value, being the median value of levoglucosan based on  
241 the values reported by all participating laboratories in the actual intercomparison.

242

### 243 1.6.4 Uncertainties of the $f_{nf}(TC_p)$ determination from $^{14}\text{C}$ analysis

244 Uncertainties of  $^{14}\text{C}(TC)$  measurements were 1–4% for the front filters and 2–10% for the pooled back  
245 filters. The uncertainties of the front filters increased upon calculation of  $^{14}\text{C}(TC_p)$ , especially for filters  
246 with high SVOC contributions. A further increase occurred when determining  $f_{nf}(TC_p)$  ( $f_{nf}$  = fraction  
247 non fossil) due to the uncertainty of the reference  $f_M$  value of pure non-fossil emissions so that the final  
248 uncertainties of the non-fossil fraction of  $TC_p$  given in Table 2a and b ranged from 0.03 to 0.09.

249 Two samples from Birkenes and two from Košetice had unrealistically high  $^{14}\text{C}$  values, for  
250 unknown reasons. This finding was confirmed when rerunning the samples at another research  
251 institute. There are other examples showing that super modern carbon can be an issue for TC measured  
252 at European rural background sites (e.g. Glasius et al., 2018). Several hypothesis were suggested with

253 respect to what are the sources of super-modern carbon in the atmosphere: e.g. emissions from nuclear  
254 power plants, waste incinerators taking care of waste from laboratories and hospitals, and crematoriums  
255 (Buchholz et al., 2013; Zotter et al., 2014). Although samples highly contaminated with super-modern  
256  $^{14}\text{C}$  are easily observed, it is not possible to determine if reasonable looking samples are free from such  
257 contamination.  $^{14}\text{C}$  contaminated measurements may lead to an overestimation of sources that emit  
258 modern carbon when performing source apportionment of the carbonaceous aerosol, as described in the  
259 current paper.

260

## 261 **1.7 Chemical transport modelling**

262 An important use of the carbonaceous aerosol Latin Hypercube Sampling (LHS) based source  
263 apportionment, is to evaluate and constrain model systems for simulating particulate matter in the  
264 atmosphere. The EMEP MSC-W model (Simpson et al., 2012; 2017 and references therein) is an Open  
265 Source chemical transport model widely used for research, within the EMEP programme, and  
266 elsewhere (e.g. Simpson et al., 2007; Bergström et al., 2012; 2014; Dore et al., 2015; Ots et al., 2016;  
267 Vieno et al., 2016). In the present study we run the EMEP model with a horizontal resolution of 50 km  
268  $\times$  50 km across Europe, using 21 vertical levels, the lowest level being approximately 50 m thick.  
269 Meteorological data from the Integrated Forecast System model (IFS; Cycle 40r1) of the European  
270 Centre for Medium-Range Weather Forecasts (ECMWF) were used to drive the model. For this study,  
271 version rv4.15 of the model was used with some modifications: The OC emissions from all sources  
272 (except wildfires and open agricultural fires, which were treated as non-volatile in order to provide a  
273 tracer of these emissions, but without adding the considerable uncertainties associated with aging of  
274 any assumed VBS components) were treated as semi-volatile, and subject to evaporation and oxidation  
275 in the gas-phase (ageing), using a volatility basis set (VBS) approach, similar to the VBS PAA scheme  
276 in Bergström et al. (2012; the PAA scheme includes gas-particle Partitioning of primary organic  
277 aerosol emissions and Aging of All semi-volatile OA components in the gas-phase). The model was  
278 run for the years 2008 and 2009, with two different emission set-ups (See Sects. 1.7.1.1 and 1.7.1.2) in  
279 order to evaluate model performance for biomass-burning derived OC and EC with these inventories.  
280 Initial and lateral boundary conditions for the EMEP model are specified for most pollutants, as in  
281 Simpson et al. (2012). For OM, the model assumes a background level of organic matter to represent  
282 OM transported into the modelling domain, or otherwise not accounted for (e.g. marine aerosol, some  
283 primary biological aerosol particles, or very aged aerosol from outside the domain). In the initial setup  
284 of Bergström et al. (2012) and Simpson et al. (2012), we used  $1.0 \text{ ug m}^{-3}$  OM, but results presented in  
285 Bergström et al. (2012) and later studies suggested that this was too high. As in Bergström et al. (2014),  
286 we assume a background concentration of particulate OM of  $0.4 \text{ ug m}^{-3}$  (with an OM/OC ratio of 2.0)  
287 near the ground.

288

### 289 **1.7.1 Emissions**

290 European residential wood burning inventories have substantial inconsistencies between countries  
291 (Denier van der Gon, 2015a; Simpson and Denier van der Gon, 2015), and several assumptions  
292 concerning volatility and oxidation-processes for such emissions are possible (e.g. Robinson et al.,



293 2007; Grieshop et al., 2009; Bergström et al., 2012; May et al. 2013a; Jathar et al., 2014; Ciarelli et al.,  
294 2017). To illustrate some of the uncertainties associated with this, two different emission set-ups were  
295 applied in the present study: A base-case run using the widely used MACC-III emission inventory, and  
296 an alternative run, denoted DT+IVOC.

297 In both cases, anthropogenic emissions (except as noted below) were based on the TNO  
298 MACC emission inventory for 2011 (Kuenen et al., 2014; Denier van der Gon et al., 2015b) with  
299 emission categories following the SNAP system, in which SNAP-2 includes non-industrial combustion,  
300 such as residential wood burning. Emissions from vegetation fires and agricultural burning were taken  
301 from the Fire INventory from NCAR version 1.5 (FINNv1.5; Wiedinmyer et al., 2014) and OC  
302 emissions from these types of fires were treated as non-volatile.

303

#### 304 **1.7.1.1 Base Case**

305 For SNAP-2, the MACC-III emissions were split into biomass burning sources (mainly wood and  
306 woody fuels) and fossil fuel sources (coal, oil etc.), using data from Kuenen (pers. comm., 2017). The  
307 emissions in MACC-III were split into five volatility bins, with saturation concentrations ( $C_{298K}^*$ , in the  
308 range 0.01–1000  $\mu\text{g m}^{-3}$ ) as shown in Table 3.

309

#### 310 **1.7.1.2 DT+IVOC Case**

311 POA and EC SNAP-2 emissions from MACC-III were scaled (except for Russia, for which the  
312 MACC\_III emissions were used also in the DT+IVOC runs) to better match the bottom-up inventory  
313 ‘DT’ from Denier van der Gon (2015a), where DT refers to data from dilution tunnels, which capture  
314 condensables (SVOC) in addition to solid particles. This causes a substantial increase in POA  
315 emissions for some countries (e.g. by more than a factor of three for Germany), but only minor for  
316 others (e.g. Norway), as discussed by Denier van der Gon, (2015a). The DT/IVOC case adds extra  
317 emissions of intermediate volatility compounds (IVOC) for all primary OA (POA) sources, as in  
318 Denier van der Gon (2015a). The split between biomass burning (non-fossil) emissions and fossil fuel  
319 based emissions for SNAP-2 was taken from the inventory of Denier van der Gon (2015a). Table 3  
320 details the volatility assumptions used for the DT+IVOC case. EC emissions from wood combustion  
321 are also different in the two different inventories (see Genberg et al., 2013, for a detailed discussion of  
322 the EC emissions in the DT emission inventory).

323

## 324 **2. Source apportionment using Latin Hypercube Sampling**

325 Source apportionment of TC into different source categories of fossil-fuel, biomass burning and  
326 remaining non-fossil carbon for OC and EC has been done with chemical and  $^{14}\text{C}$  tracers. This  
327 methodology, which is very similar to that used in Yttri et al. (2011a), was originally developed for the  
328 CARBOSOL project (Gelencsér et al., 2007), and has been refined over the years, and applied in  
329 several Nordic studies (Szidat et al., 2009, Yttri et al., 2011a, b, Glasius et al., 2018). In summary:  
330 Measurements of levoglucosan are used as a tracer of wood-burning emissions ( $\text{TC}_{\text{bb}} = \text{OC}_{\text{bb}} + \text{EC}_{\text{bb}}$ ;  
331  $\text{OC}_{\text{bb}}$  includes primary and secondary OC) and the  $^{14}\text{C}$  isotopic ratio ( $F^{14}\text{C}$ ), along with measured OC  
332 and EC, and assumed emission ratios (e.g.  $\text{TC}_{\text{bb}}/\text{levoglucosan}$  and  $\text{OC}_{\text{bb}}/\text{TC}_{\text{bb}}$  from wood combustion,

333 or OC/EC ratios from fossil-fuel combustion), to assign the remaining carbon between fossil-fuel  
334 sources and secondary organic aerosol sources. When available (as in Yttri et al., 2011a), mannitol and  
335 cellulose can be used as tracers of primary biological aerosol particles ( $OC_{PBAP}$ ) derived from fungal  
336 spores ( $OC_{pbs}$ ) and plant debris ( $OC_{pbc}$ ), respectively. Total carbon is in this way split into  $TC_{bb}$ ,  
337  $OC_{PBAP}$ ,  $TC_{ff}$  ( $= OC_{ff} + EC_{ff}$ , from fossil-fuel sources;  $OC_{ff}$  includes primary and secondary OC), and  
338 finally, any remaining modern-carbon is labeled  $OC_{mf}$ , which typically is dominated by  $OC_{BSOA}$   
339 (biogenic secondary organic aerosol), but might also include other sources, such as SOA from biomass  
340 burning and emissions related to cooking (Mohr et al., 2009; Crippa et al., 2014). Note that Crippa et  
341 al. (2014) did not find any influence of cooking at European rural background sites doing a source  
342 apportionment study of the carbonaceous aerosol based on Aerosol Mass Spectrometer (AMS)  
343 measurements. The relationship between any tracer and its derived TC component is very uncertain,  
344 thus an uncertainty distribution of allowed parameter values for all important emission ratios or  
345 measurement inputs is assigned. In order to solve the system of equations, allowing for the multitude of  
346 possible combinations of parameters, an effective statistical approach known as Latin-hypercube  
347 sampling is used, which is comparable to Monte Carlo calculations. In brief, central values with low  
348 and high limits are associated to all uncertain input parameters. These factors are combined using LHS  
349 in order to generate thousands of solutions for the source-apportionment. All valid combinations of  
350 parameters (i.e. excluding those producing negative solutions) are condensed in frequency distributions  
351 of possible solutions. Extensive discussion of the choices behind the factors used, and their  
352 uncertainties, can be found in earlier related studies (Yttri et al., 2011a, Szidat et al., 2009 Gelencsér et  
353 al., 2007, Simpson et al., 2007). The result of this analysis consist of so-called central-estimates of the  
354 TC components (i.e. the 50th percentile), as well as the range of possibilities allowed by the LHS  
355 calculation, e.g. expressed as the 10th and 90th percentiles of the solutions.

356 There are two major differences in the data available for this study compared to Yttri et al.  
357 (2011a, b), requiring modification of the methodology and factors used: i) For the present study, we  
358 have no data to estimate the fractions of PBAP and BSOA, thus  $OC_{mf}$  comprises both  $OC_{BSOA}$ ,  $OC_{PBAP}$   
359 and indeed all other non-fossil sources of OC; ii) The geographical scope of the current study is wider,  
360 and in particular biomass burning in southern Europe involves different tree species than those used in  
361 the Northern European studies of Yttri et al. (2011a,b) or Szidat et al. (2009).

362 Concerning item (i), we require a range of values of the  $F^{14}C$  value associated with  $OC_{mf}$ . In  
363 Yttri et al. (2011a,b) we used 1.055 for BSOA and PBAP associated with plant debris, but allowed  
364  $F^{14}C$  for spores to vary between 1.055 and 1.25, reflecting the utilization of older carbon-stocks by  
365 fungi. As noted above, we have no direct tracers for BSOA or PBAP, but a few studies allow a general  
366 estimate. Winiwarter et al. (2009) suggested that fungal spores were likely the dominant contributor to  
367 PBAP across Europe. Results scaled for Europe indicated a contribution of PBAPs to  $PM_{10}$   
368 concentrations in the low percentage range, with a maximum in summer when  $PM_{10}$  concentration  
369 levels are small. Similarly, Bauer et al. (2008) had spores contributing 6% to OC in spring and 14% in  
370 summer at a suburban site, whereas the corresponding contribution to  $PM_{10}$  was 3% (spring) and 7%  
371 (summer). In Norway, Yttri et al. (2011a) found spores and debris contributing 18% and 6%,  
372 respectively, to TC at a rural site in summer, with 0.5% and 7% respectively in winter. For comparison,

373 BSOA contributed 56% and 11% of TC in summer and winter at the actual site. Hence, spores and  
374 plant debris are likely to make a certain contribution, but are unlikely to dominate OC<sub>nf</sub>. In order to  
375 account for this, we allow F<sup>14</sup>C to vary between 1.055 to 1.100 in the present study.

376 Concerning item (ii), the main effect is likely to be on the assumed TC/levoglucosan ratios  
377 used in the LHS method. In Yttri et al. (2011a,b) we used low, central and high values of 11, 15 and 17  
378 for PM<sub>10</sub>, or 7.6, 12, and 14 for PM<sub>2.5</sub>, factors derived from ambient Norwegian data, and modified to  
379 be appropriate to the QBQ sampling used for the LHS. These values also seem to be consistent with the  
380 study of Elsasser et al. (2012), which reported OC/levoglucosan values from filter samples of about  
381 10–17 for Augsburg, Germany. Inclusion of EC would give TC<sub>bb</sub>/levoglucosan values at the high end  
382 of our assumed range.

383 We have no equivalent data for southern Europe, but a simple examination of the data in Table  
384 2 suggests that levoglucosan levels can be high at the Italian sites, and assuming high ratios of  
385 (TC/levoglucosan)<sub>bb</sub> in emissions would result in LHS-estimated TC<sub>bb</sub> higher than observed TC, which  
386 clearly is impossible. Gilardoni et al., (2011) used (OC/levoglucosan)<sub>bb</sub> of 4 to 13, then (OC/EC)<sub>bb</sub> of 1  
387 to 20, whereas Zotter et al. (2014) observed (OC/levoglucosan)<sub>bb</sub> of 7.8±2.7 and (OC/EC)<sub>bb</sub> of 8.6±2.9  
388 for Southern Switzerland, which is close to the Italian site Ispra. It isn't obvious how to derive  
389 (TC/levoglucosan)<sub>bb</sub> from these values, but low values are clearly suggested by these choices.

390 In order to allow for this possibility, we have extended the lower range of our  
391 (TC/levoglucosan)<sub>bb</sub> ratio to be 5, thus using low, central and high of 5, 15 and 17 for PM<sub>10</sub>. This  
392 actually made very little difference to the LHS solutions for central and northern Europe, but allowed  
393 more solutions for the Italian sites.

394 No attempts to run LHS were possible for samples with unrealistically high <sup>14</sup>C(TC) values,  
395 affecting two samples each from Birkenes and Košetice. No valid solution was obtained for five of the  
396 samples collected at Ispra, two at Melpitz, one at Birkenes and one at Payerne. This may be an  
397 indication of problems with the samples (e.g. artefacts or contaminated <sup>14</sup>C(TC) values), or with the  
398 assumptions underlying LHS breaking down. Nevertheless, LHS-based source apportionment was  
399 obtained for 29/35 samples in fall and for 29/36 in winter/spring.

400

### 401 3. Results

#### 402 3.1 Ambient concentrations of the carbonaceous aerosol

403 Concentrations of elemental carbon (EC), positive-artefact-corrected particulate organic carbon (OC<sub>p</sub>),  
404 organic carbon on back filters (OC<sub>B</sub>), positive-artefact-corrected particulate total carbon (TC<sub>p</sub>) and  
405 levoglucosan, as well as the EC/TC<sub>p</sub> ratio and the f<sub>nf</sub>(TC<sub>p</sub>) fraction observed during the fall 2008 and  
406 the winter/spring 2009 intensive measurement periods, are presented in Table 2.

407

##### 408 3.1.1 EC and OC<sub>p</sub>

409 The mean (±SD; standard deviation) EC concentration (0.64±0.58 μg C m<sup>-3</sup> in fall; 0.58±0.50 μg C m<sup>-3</sup>  
410 in winter/spring) was quite similar to the annual mean (±SD) concentration reported for 12 European  
411 rural background (EMEP) sites in 2002–2003 (0.66±0.39 μg m<sup>-3</sup>; Yttri et al., 2007a), but slightly less  
412 than the winter time mean (0.79±0.83 μg C m<sup>-3</sup>; *ibid.*). Although thermal-optical analysis was used

413 both in the present study and in that by Yttri et al. (2007a), different temperature protocols can cause  
414 substantial differences in the OC/EC split. However, only a minor difference was observed with respect  
415 to the EC/TC ratio when analyzing the “8785 Air Particulate Matter On Filter Media” reference  
416 material from NIST using the EUSAAR-2 protocol and the NIOSH derived protocol (Yttri et al.,  
417 2007a). The mean EC concentration varied by a factor of ~15 between sites both in fall and in  
418 winter/spring, with concentrations at Birkenes and Mace Head (North-western Europe) being  
419 substantially lower than for continental European sites, particularly compared to the southern sites  
420 (Montelibretti, Ispra and K-puszta). A pronounced North-to-South gradient for EC, and OC, has  
421 previously been reported by Yttri et al. (2007a), reflecting diluted emissions from major source regions  
422 in continental Europe reaching distant and less polluted sites on the outskirts of Europe. In addition, the  
423 proximity to the coast causes efficient ventilation and air mass mixing at the sites Birkenes and Mace  
424 Head.

425         The mean ( $\pm$ SD) OC<sub>p</sub> concentrations in fall ( $2.9\pm 3.1 \mu\text{g C m}^{-3}$ ) and winter/spring ( $2.8\pm 2.3 \mu\text{g}$   
426  $\text{C m}^{-3}$ ) were almost identical. A few, high concentration samples at the sites Montelibretti, Ispra and K-  
427 puszta influenced the winter/spring mean, as evident from the mean-to-median ratio of 1.6 compared to  
428 1.2 in fall. Mean ( $\pm$ SD) OC<sub>p</sub> concentrations reported here were slightly lower than the annual ( $3.4\pm 3.6$   
429  $\mu\text{g C m}^{-3}$ ) and winter time ( $3.7\pm 4.4 \mu\text{g C m}^{-3}$ ) mean OC concentrations reported for EMEP sites in  
430 2002–2003 (Yttri et al., 2007a). Differences in sampling time, temperature protocol, and sampling  
431 approach [the current study accounted for the positive sampling artefact of OC, whereas Yttri et al.,  
432 (2007) did not], are likely to explain the (minor) differences in the OC concentration between the two  
433 studies. If we allow for a positive artefact of similar magnitude as that observed in the present study,  
434  $16\pm 8 \%$  in fall and  $17\pm 9 \%$  in winter/spring, also for the Yttri et al. (2007a) study, levels would be  
435 fairly similar.

436         A North-to-South gradient was observed for OC<sub>p</sub> as for EC, which was less prominent in fall  
437 compared to winter/spring.

438

### 439 **3.1.2 EC/TC ratio**

440 The EC/TC<sub>p</sub> ratio ranged from 11 to 28 % in fall, and from 14 to 24 % in winter/spring. No pronounced  
441 shift in the EC/TC<sub>p</sub> ratio was observed between the two periods, except for the Norwegian site  
442 Birkenes, for which the EC/TC<sub>p</sub> ratio was 11% in fall and 21% in winter/spring.

443

### 444 **3.1.3 Levoglucosan**

445 The mean concentration of the wood burning tracer levoglucosan varied by more than a factor of 50  
446 between sites, both in fall and in winter/spring. There was a pronounced North-to-South gradient, as for  
447 OC<sub>p</sub> and EC and the mean concentration was higher in winter/spring than in fall at all sites, except  
448 Košetice and Mace Head. The levoglucosan level is within the range reported for six European rural  
449 background sites ( $2.7\text{--}1220 \text{ ng m}^{-3}$ ) by Puxbaum et al. (2007), and for Montelibretti, Ispra, and K-  
450 puszta, levels equaled the concentration range reported for urban areas in winter (Szidat et al., 2009).

451

### 452 3.1.4 $f_{\text{nf}}(\text{TC}_p)$ from $^{14}\text{C}$ analysis

453 The non-fossil fraction of  $\text{TC}_p$  (i.e.  $f_{\text{nf}}(\text{TC}_p)$ ) of individual aerosol filter samples varied from 0.51 to  
454  $>1.00$ . Two samples from Birkenes and two samples from Košetice showed such high  $^{14}\text{C}(\text{TC})$  results  
455 that the corresponding  $f_{\text{nf}}(\text{TC}_p)$  resulted in levels as high as 1.68. These unreasonable values point to an  
456 anthropogenic bias of local  $^{14}\text{C}$  emissions, which distort the source apportionment. Similar cases have  
457 occasionally been observed at other sites, mainly caused by local pharmaceutical facilities with  
458 incineration units for  $^{14}\text{C}$ -labelled waste (Buchholz et al., 2013; Zotter et al., 2014). In some cases, the  
459 specific source could not be identified, as for Birkenes and Košetice. Consequently, the biased values  
460 were excluded from further analysis. The remaining results from these two sites were included, as they  
461 correspond well with values from the other sites, although their reliability remains unclear.

462 Mean  $f_{\text{nf}}(\text{TC}_p)$  values ranged from 0.61–0.91 for the individual sites, including both fall and  
463 winter/spring. These values correspond to those reported at five European rural and remote sites in  
464 summer and winter by Gelencsér et al. (2007) and to an urban and a rural site in Norway (Yttri et al.,  
465 2011a), but are higher compared to rural and urban sites in Switzerland and Sweden during summer  
466 and winter (Szidat et al., 2009). The seasonal variation was typically not pronounced, although most  
467 sites experienced the highest  $f_{\text{nf}}(\text{TC}_p)$  values in winter/spring. The exceptions were Montelibretti, at  
468 which  $f_{\text{nf}}(\text{TC}_p)$  was noticeably higher in winter/spring (0.80) compared to fall (0.61), and Košetice at  
469 which  $f_{\text{nf}}(\text{TC}_p)$  was higher in fall 2008 (0.86) compared to winter/spring 2009 (0.69).

470

## 471 4. Discussion

472 Results from the carbonaceous aerosol source apportionment (Figure 2; Table 4) show a variability in  
473 the carbonaceous aerosol source composition, both as a function of season and location. The results  
474 from the source apportionment analyses are discussed in detail in sections 4.1–4.6. Calculated  
475 concentrations and relative contributions typically showed little variability between samples collected  
476 within each season for each of the nine sites. Hence, comparing results based on calculated mean  
477 values can be argued for. The results presented are complementary to those of Gelencsér et al. (2007),  
478 Genberg et al. (2011) and Yttri et al. (2011a,b), as the same (or similar in the case of Genberg et al.)  
479 software/methodology is applied, but for a wider range of sites, and with updated emission ratios  
480 (Zotter et al., 2014) for the central and southern European sites.

481 A major difficulty for all modelling work is the complexity of organic aerosol, in terms of  
482 emissions, formation mechanisms, and deposition processes (e.g. Hallquist et al., 2009; Hodzic et al.,  
483 2016). Considering emissions, we can note that Denier van der Gon (2015a) utilized a specially  
484 developed map of residential wood combustion sources, which however was specific to that study and  
485 not utilized in subsequent spatial mapping of emissions. Studies in the United Kingdom and Norway  
486 have also cast doubt on the accuracy of spatial distributions of emissions (Ots et al., 2016; López-  
487 Aparicio et al., 2017), which inevitably causes problems for modelling. Compounding the difficulties,  
488 different SOA schemes give different answers, as we explored in detail in Bergström et al. (2012).  
489 However, sensitivity tests performed as part of the studies by Bergström et al. (2012), Simpson et al.  
490 (2012) and Denier van der Gon et al. (2015a) have shown that differences in OM caused by emissions  
491 assumptions are larger than those caused by e.g. volatility assumptions. We have used two sets of

492 assumptions (base-case and DT+IVOC) in our work, which we believe span a reasonable range of  
493 possibilities. Given these difficulties, it is not surprising that model results can show large scatter  
494 compared to measured values. However, we have also shown in several studies (Bergström et al., 2012,  
495 Genberg et al., 2011, 2013, Denier van der Gon et al., 2015a), that the model results do improve  
496 compared to observations when condensables are treated in a more uniform matter, and the current  
497 study is consistent with this.

498

#### 499 **4.1 Carbonaceous aerosol from fossil-fuel sources and biomass burning**

500 Fossil fuel combustion was the major source of EC at all sites in fall, accounting for 6% to 22% of TC<sub>p</sub>,  
501 whereas EC from biomass burning was < 8% at all sites. The influence of EC<sub>ff</sub> was particularly  
502 pronounced at the sites Montelibretti (22%) and Lille Valby (21%), which for Montelibretti could be  
503 due to the proximity of the Rome metropolitan area, with 3.7 million inhabitants. Lille Valby is a semi-  
504 rural site, and thus could be more influenced by e.g. vehicular particulate emissions. Fossil fuel  
505 combustion continued to be the most important source of EC in winter/spring for the five northernmost  
506 sites, whereas there was a shift towards biomass burning for the four southernmost sites. The relative  
507 contribution of EC<sub>bb</sub> and EC<sub>ff</sub> to TC<sub>p</sub> in winter/spring was ≤ 10%, except at the sites Lille Valby,  
508 Melpitz and Birkenes that experienced relative contributions of EC<sub>ff</sub> exceeding 10%. EC<sub>bb</sub> was a more  
509 abundant fraction of TC<sub>p</sub> in winter/spring compared to fall at all sites. The picture was less consistent  
510 for EC<sub>ff</sub>, with a higher relative contribution in fall at the four southernmost sites, and for Lille Valby,  
511 and a higher fraction in winter/spring for the four other sites.

512 Biomass burning was the major anthropogenic source of OC at most sites in fall, accounting  
513 from 5% to 36% of TC<sub>p</sub>, whereas OC from fossil fuel ranged from 8% to 21%. The exceptions were  
514 Birkenes and Mace Head for which OC<sub>ff</sub> dominated with 16% and 21%, respectively. At Montelibretti,  
515 OC<sub>bb</sub> and OC<sub>ff</sub> made equally large contributions to TC<sub>p</sub> (18% each).

516 In winter/spring, biomass burning was the major anthropogenic source of OC at all sites  
517 except at Mace Head, constituting 11% to 46% of TC<sub>p</sub>, whereas the range for OC<sub>ff</sub> was 10% to 23%.  
518 OC<sub>bb</sub> was more abundant in winter/spring compared to fall for all sites but Mace Head, whereas there  
519 was no consistent pattern observed for OC<sub>ff</sub>. There was a general tendency that OC<sub>bb</sub> became less  
520 abundant along a South-to-North transect, as seen for EC<sub>bb</sub>.

521 Biomass burning had a pronounced influence at most sites already in the first week of  
522 sampling in fall (17–24 September): EC<sub>bb</sub> and OC<sub>bb</sub> contributed a substantial 57% of TC<sub>p</sub> at K-puszt  
523 and 54% at Ispra, 34% and 37% at Melpitz and Payerne, respectively, whereas it ranged from 21–29%  
524 for the sites Mace Head, Košetice and Lille Valby. Birkenes was the only sites where wood burning  
525 made a minor contribution (6%) this week. Model calculations suggest that wild and agricultural fires  
526 were of minor importance at all sites for the actual week, with the highest model calculated  
527 concentration (0.02 μg C m<sup>-3</sup>) at Ispra and Lille Valby, corresponding to 3% and 5% of the modelled  
528 TC<sub>bb</sub> (See section 4.2). Hence, residential wood burning appears to be the source of EC<sub>bb</sub> and OC<sub>bb</sub>,  
529 although given the uncertainties of emission estimates for wild and agricultural fires, such sources  
530 cannot be ruled out. The mean temperature during the first week of sampling was not noticeably lower

531 than seen for the rest of the sampling period. Still, it was the week with the lowest mean temperature  
532 for the sites K-puszta, Payerne and Košetice.

533

#### 534 **4.2 Wild and agricultural fire contribution**

535 Wild and agricultural fires are major sources of carbonaceous aerosol (Bond et al., 2004), but with  
536 large regional, seasonal and annual differences in emissions and occurrence (Hao et al., 2016; Korontzi  
537 et al., 2006). Agricultural waste burning is banned in most European countries, nevertheless, remote  
538 sensing data show such fire events in several countries, including those with a ban (Korontzi et al.,  
539 2006), and it appears particularly frequent in Eastern Europe (e.g. Belarus and the Ukraine), in western  
540 parts of Russia, and in Central Asia. In most cases when natural vegetation catches fire in Europe, this  
541 is due to human activity (Winiwarter et al., 1999).

542 Incidences of wild and agricultural fires that severely deteriorate air quality in large parts of  
543 Europe are regularly reported e.g. by Yttri et al. (2007a) for 2002, by Stohl et al. (2007) for 2006, and  
544 Diapouli et al. (2014) for 2010. The two periods discussed in the present study partly coincide with the  
545 time when concentrations from wild and agricultural fires peak in Europe (Korontzi et al., 2006).  
546 Levoglucosan by itself cannot differentiate between emissions from residential wood burning and wild  
547 and agricultural fires. Hence, we have used modelled concentrations to address the relative contribution  
548 of TC from wild fires and agricultural fires ( $TC_{wf}$ ) to the sum of TC from residential wood burning  
549 ( $TC_{bb}$ ) and  $TC_{wf}$  for the two sampling periods.

550 There was an influence from wild and agricultural fires at all sites, with a higher mean  
551 contribution in fall ( $TC_{wf} = 0.05 \mu\text{g C m}^{-3}$ ), corresponding to 9–16% (for base-case, or DT+IVOC) of  
552 modelled  $TC_{bb}$ , than in winter/spring ( $TC_{wf} = 0.015 \mu\text{g C m}^{-3}$ ), corresponding to 2–4% of modelled  
553  $TC_{bb}$ .  $TC_{wf}$  were typically low also on a weekly basis, but for the last week of sampling in fall, a  
554 noticeable contribution was calculated for Ispra (34%), K-puszta (31%), and Montelibretti (16%).

555 The major conclusion to be drawn from these results is that the model predicts that wild and  
556 agricultural fires make minor contributions to the biomass burning carbonaceous aerosol at the sites  
557 addressed, and that residential wood burning is the major source.

558

#### 559 **4.3 Remaining non-fossil sources of organic carbon**

560 Remaining non-fossil sources of OC ( $OC_{mf}$ ) are typically associated with biogenic secondary organic  
561 aerosol ( $OC_{BSOA}$ ) and primary biological aerosol particles ( $OC_{PBAP}$ ), however there are anthropogenic  
562 sources of modern carbon as well, as discussed in detail by Yttri et al. (2011a). Here, we discuss the  
563 results obtained for  $OC_{mf}$  as if natural sources are dominating.

564 The  $OC_{mf}$  level varied more widely in winter ( $0.1\text{--}2.2 \mu\text{g C m}^{-3}$ ) than in fall ( $0.6\text{--}3.0 \mu\text{g C m}^{-3}$ )  
565 (Figure 2) and corresponds well with levels reported for the European rural background environment  
566 (Gelencsér et al., 2007; Genberg et al., 2011; Yttri et al., 2011a,b). The spatial distribution of  $OC_{mf}$   
567 equaled that of  $OC_p$ , with high concentrations at the southernmost sites and decreasing levels along a  
568 South-to-North transect.

569  $OC_{mf}$  levels were higher in fall compared to winter/spring for all sites, but the difference  
570 varied from minor at most sites, moderate at the continental sites Košetice and Payerne, and substantial

571 at the Norwegian site Birkenes. Studies consistently point towards BSOA as the major contributor to  
572 OC<sub>mf</sub> in Europe (e.g., Simpson et al., 2007; Bessagnet et al., 2008; Yttri et al., 2011a); e.g. Gelencsér et  
573 al. (2007) showed that BSOA in PM<sub>2.5</sub> was 1.6–12 times higher in summer than in winter for six  
574 European rural background sites. Hence, the observed pattern could partly be explained by a higher  
575 formation rate of BSOA in fall, propelled by larger emissions of BSOA precursors and a higher  
576 ambient temperature (See Table 1 ambient temperature values). In the present study, PM<sub>10</sub> filter  
577 samples were collected (except at Mace Head, where PM<sub>2.5</sub> was collected). Consequently, primary  
578 biological aerosol particles (PBAP), typically residing in the coarse fraction of PM<sub>10</sub> (e.g., Yttri et al.,  
579 2007b; Kourtchev et al., 2009; Bozzetti et al., 2016), could contribute to OC<sub>mf</sub> as well. In Scandinavia,  
580 PBAP peak in summer and fall, reflecting the vegetative season and the absence/presence of a snow  
581 cover (Yttri et al., 2007a,b; 2011a,b), and summer time OC<sub>PBAP</sub> concentrations (PM<sub>10</sub>) being 7–8 times  
582 higher than in winter, has been reported for two Norwegian sites (Yttri et al., 2011a). In continental  
583 Europe, the vegetative season is longer than in Scandinavia and a permanent snow cover is associated  
584 with high altitude regions and rare occasions, lasting for short periods, in low altitude regions. Hence,  
585 one could speculate that there is a PBAP emission flux in continental Europe in the heating season,  
586 which is comparatively larger than that observed in Scandinavia. We find support of this view in the  
587 study by Waked et al. (2014), which showed a tail of PBAP and episodes with high PBAP  
588 concentrations in winter for an urban background site in Northern France. Knowledge of PBAP  
589 concentrations in Europe is limited, thus we can only speculate about how much of OC<sub>mf</sub> in the present  
590 study is due to PBAP. A noticeable 20–32% contribution of OC<sub>PBAP</sub> to TC<sub>p</sub> was found at four Nordic  
591 rural background sites in late summer (Yttri et al., 2011b). Similar figures (OC from primary biogenics  
592 constituting up to 33% of OC in PM<sub>10</sub>) were reported for the densely populated region of Berlin in  
593 north-eastern Germany (Wagener et al., 2012) in late summer and fall. Gelencsér et al. (2007) and  
594 Gilardoni et al. (2011) both reported levels of OC associated with PBAP for an entire year for the  
595 European rural background environment, finding that the relative contribution to total carbon was < 5%  
596 in summer and < 8% in winter. However, both studies relied on PM<sub>2.5</sub> samples, likely excluding the  
597 majority of PBAP. Further, Gelencsér et al. (2007) accounted for plant debris only when measuring  
598 cellulose, whereas Gilardoni et al. (2011) only accounted for fungal spores, measuring  
599 arabitol/mannitol. Waked et al. (2014) found that 17% of the OC was attributed to OC<sub>PBAP</sub> on an annual  
600 basis for an urban background site, with substantially higher concentrations in summer (37%) and fall  
601 (20%) compared to winter (7%) and spring (6%). At the rural background site Payerne, Bozzetti et al.  
602 (2016) found that PBAP, mainly from plant debris, equaled the contribution of SOA to organic matter  
603 in PM<sub>10</sub> in summer.

604 The non-fossil signal was typically most pronounced in fall, with the highest relative share (52 –  
605 69%) observed for the two low loading sites situated on the outskirts of Europe (Birkenes and Mace  
606 Head) and the lowest for the highest loading site, Ispra (23%). Note that OC<sub>mf</sub> obtained for Mace Head  
607 is a conservative estimate, as PBAP typically residing in the coarse fraction is not accounted for, as  
608 PM<sub>2.5</sub> filter samples were collected at this site. Nevertheless, OC<sub>mf</sub> was the major fraction at Mace  
609 Head, regardless of season; hence, our conclusions would not change if the filter samples had PM<sub>10</sub> cut-  
610 off size. A pronounced non-fossil signal (52 – 54%) was seen for the continental sites Košetice and



611 Payerne as well, whereas the relative share ranged between 38% and 48% for the remaining sites. Non-  
612 fossil OC was by far the major source of OC at all sites in fall, except at Ispra, for which biomass  
613 burning dominated. The non-fossil signal decreased, or remained unchanged, for all but one site going  
614 from fall to winter/spring, but the reduction was substantial only at the Norwegian site Birkenes (a  
615 factor of  $\sim 2$ ), at Payerne and Košetice (a factor of 1.5–1.7), and at Melpitz (a factor of 1.5). Still, non-  
616 fossil OC was the major source of OC at five sites even in winter/spring, K-pusztta, Košetice, Lille  
617 Valby, Mace Head and Birkenes. It has been suggested that increased condensation due to lower  
618 temperatures could be an efficient way of forming BSOA even in winter (Simpson et al., 2007). It is  
619 however difficult to argue for such a hypothesis only by looking at the observed ambient air  
620 temperatures during the winter/spring period. Another possibility is that some of the remaining non-  
621 fossil OC may be secondary organic aerosol formed from volatile or semi-volatile OC emitted from  
622 wood burning.  $OC_{bb}$  determined based on levoglucosan may not include all SOA formed after aging of  
623 the gas-phase emissions, even if the emission ratios were derived from ambient measurements and  
624 likely include condensed vapors and secondary products.

625

#### 626 **4.4 Natural versus anthropogenic sources of carbonaceous aerosol**

627 In the current study, results obtained for  $OC_{mf}$  are discussed as if natural sources are dominating,  
628 despite that anthropogenic sources can make a certain contribution, e.g. from cooking emissions and by  
629 anthropogenic enhancement of BSOA formation. EC and OC emitted from combustion of fossil fuel  
630 and biomass are considered entirely anthropogenic, as we define wild fires as anthropogenic.

631 In fall, the anthropogenic and natural influences were of comparable magnitude at most sites.  
632 Exceptions were Birkenes, with a clearly larger natural contribution (69%), and Ispra, with a larger  
633 anthropogenic contribution (77%), the latter affected by regional air pollution in the strongly polluted  
634 Po Valley region. For the other sites, the anthropogenic fraction ranged from 46 – 62% and from 38 –  
635 54% for the natural fraction. Increased condensation due to lower temperatures can be an important  
636 source of BSOA in fall and winter, which could outweigh the effect of high temperature and increased  
637 terpene emissions in summer (Andersson-Sköld and Simpson, 2001. Simpson et al., 2007). Further,  
638 PBAP can make a pronounced contribution in fall both in Scandinavia (Yttri et al., 2007a,b; 2011a,b)  
639 and in continental Europe (Waked et al., 2014; Bozzetti et al., 2016), and the fall peak of the North-  
640 Eastern Atlantic Ocean phytoalgal bloom takes place during the period in question, likely contributing  
641 with marine PBAP at Mace Head (Ceburnis et al., 2011).

642 In winter/spring, anthropogenic sources dominated at all sites (60 – 78% anthropogenic),  
643 except for Mace Head (37%). Ispra had the most pronounced anthropogenic contribution of all sites  
644 also in winter/spring (78%), and it was largely unchanged from that observed in fall. Three of the four  
645 sites experiencing a high natural influence in fall, (Birkenes, Košetice and Payerne) saw a major  
646 increase in the anthropogenic contribution going from fall to winter/spring. This was attributed to a  
647 substantial reduction in natural sources, accompanied by an increase in the anthropogenic sources,  
648 being primarily biomass burning at Payerne and Birkenes and fossil fuel sources at Košetice.  
649 Residential wood burning is considered a decentralized source in Europe, and emissions from local  
650 sources can be substantial in winter (Szidat et al., 2007). A certain local contribution could also be

651 speculated for Košetice, as small coal-fired ovens still are common in rural areas in Eastern Europe  
652 (Spindler et al., 2012).

653

#### 654 **4.5 Modelling contributions from biomass burning**

655 The EMEP MSC-W model was run with two different emission and SOA modelling set-ups (a base-  
656 case and DT+IVOC) in order to reflect (to some extent) the very large uncertainties in both emissions  
657 and atmospheric processing of the primary organic aerosol (POA) (see section 1.7). The model results  
658 were compared with that of the LHS analysis discussed above. In the following, model results that are  
659 within the 10–90 percentile range of the LHS analysis are considered as being in “agreement” with the  
660 measurements. Results outside this (fairly wide) concentration range are considered as under or over  
661 estimations.

662 Modelled  $OC_{bb}$  and  $EC_{bb}$  concentrations were compared to the LHS source apportionment  
663 results for each sample individually in Figure 3, and as averages over the measurement periods in Table  
664 4. The base-case model simulations underestimated  $OC_{bb}$  severely at most sites (Figure 3a). The only  
665 exception was Birkenes, for which the model slightly overestimated the LHS-derived estimates (the  
666 modelled  $OC_{bb}$  were within the LHS 10–90 percentile range for 3/5 weeks, whereas 2/5 weeks were  
667 overestimated). For the other sites, the mean underestimation of the LHS 10-percentile for  $OC_{bb}$  ranged  
668 from –26% at Lille Valby to –84% at Payerne.

669 The model results for  $OC_{bb}$  were clearly better with the DT+IVOC emission set-up (Figure  
670 3b), than for the base-case, at all sites except Birkenes and Lille Valby. For Košetice and Payerne, the  
671 modelled  $OC_{bb}$  was within the LHS range for a majority of the samples and the underestimation of  
672  $OC_{bb}$  was smaller than with the base-case for Ispra, Montelibretti, K-puszta and Melpitz. A few  
673 individual  $OC_{bb}$  measurements were, however, clearly overestimated with the DT+IVOC setup (one  
674 sample each for Melpitz, K-puszta and Lille Valby).

675 The results for  $EC_{bb}$  roughly split in two groups for the base-case (Figure 3c): At Birkenes and  
676 Lille Valby, the  $EC_{bb}$  concentrations were overestimated by the model most of the time; only for one  
677 sample at each site did the model  $EC_{bb}$  fall within the LHS-range. The average overestimation of the  
678 LHS 90-percentile was 69% at Lille Valby and 43% at Birkenes. At the other sites,  $EC_{bb}$  was  
679 underestimated (with a few exceptions), with an average underestimation ranging from –34%  
680 compared to the LHS 10-percentile at Melpitz to –84% at Mace Head. For the two Italian sites the  
681 average underestimation was –38%, whereas it was –39% at K-puszta and Košetice and –60% at  
682 Payerne.

683 The DT+IVOC model results were clearly better for  $EC_{bb}$ , except for the Italian sites and K-  
684 puszta where the  $EC_{bb}$  underestimation was larger due to lower  
685 emissions in the inventory of Denier van der Gon et al. (2015a).  $EC_{bb}$  was largely overestimated at the  
686 Scandinavian sites, but not as much as for the base-case emissions. The modelled  $EC_{bb}$  was within the  
687 10–90 percentile LHS range for five of the weeks at Košetice and Payerne using the DT+IVOC  
688 emissions, but there was still a tendency that levels were underestimated (one week was underestimated  
689 at Košetice, two at Payerne). For Melpitz the modelled  $EC_{bb}$  was within the LHS range for 3/6 weeks  
690 (two weeks were underestimated and one overestimated).

691 The present comparison of modelled and LHS-derived biomass burning carbonaceous aerosol  
692 concentrations, indicates that the base-case setup with the TNO MACC-III emission inventory, which  
693 is similar to official EMEP PM<sub>2.5</sub> emissions estimates, likely underestimates emissions from residential  
694 wood burning substantially in large parts of Europe. This is in line with the findings of Denier van der  
695 Gon (2015a), and reflects that emissions are established following national practice that is inconsistent  
696 between countries. Note that the inventory POA emissions were distributed across different volatility  
697 classes for the DT+IVOC emissions, as for a typical VBS treatment, whereas we did not add IVOC to  
698 the MACC-III emissions in our base-case. Although the DT+IVOC emission setup with updated wood  
699 burning emissions and extra IVOC improved the model results, large uncertainties still remain, and it  
700 cannot be excluded that wood burning emissions in some parts of Europe may be considerably larger  
701 than that estimated by Denier van der Gon et al. (2015a).

702

#### 703 **4.6 Influence of long-range transport**

704 The issue of long-range transport into Europe is important for some pollutants (especially ozone, e.g.  
705 Fiore et al., 2009, or carbon monoxide from forest fires, e.g. Forster et al., 2001). However, many years  
706 of measurements and modelling analyses support our assumption that the most likely sources of  
707 carbonaceous aerosols in our study are from Europe. For example, many years of analysis of aerosols at  
708 Mace Head on the west coast of Ireland give little evidence for aerosol transport from North America,  
709 with most organic matter (OM) assigned to marine or European sources (O'Dowd et al., 2014).  
710 Emissions from major wildfires in Eastern Europe explained the highest OC and EC concentrations at  
711 Birkenes in 2001 – 2015, as did episodes of air pollution carrying the hallmark of long-range transport;  
712 i.e., elevated levels of secondary inorganic aerosol and air masses transported at low altitude over  
713 major emission regions in Central and Eastern Europe (Yttri et al. in prep.). Meanwhile, elevated  
714 concentrations of equivalent black carbon (eBC) from fossil fuel sources (eBC<sub>ff</sub>) and from biomass  
715 burning (eBC<sub>ff</sub>) at Birkenes were associated exclusively with source regions in continental Europe  
716 (Yttri et al., in prep). Consequently, long-range transport is of major importance for elevated  
717 concentrations of carbonaceous aerosol at Birkenes, but sources are confined to the European  
718 continent.

719 Further, modelling by Simpson et al. (2007) showed that observed levels of OC and EC could be  
720 reproduced quite well over a 2-year period (CARBOSOL study) at two sites on the western coast of  
721 Europe, Mace Head in Ireland, and Aveiro in Portugal, with no suggestion of missing background  
722 sources in the model. Tsyro et al. (2007) examined the EC concentrations for the same study, and  
723 showed that European forest fires only had significant impacts for a few samples. We note that the  
724 modelling domain we use is rather large, covering all of Europe from approximately 40 degree W to 60  
725 degree E and 30-90 degree N, such that we capture all major sources and air mass circulations within  
726 several days of transport. Global model results from the EMEP model (e.g. McFiggans et al., 2019)  
727 also suggest that OM generated over North America makes only a small contribution to European  
728 particulate matter levels.

729

## 730 5 Conclusions

731 Source apportionment of carbonaceous aerosol was conducted at nine European rural background sites  
732 for a fall period in 2008 and a winter/spring period in 2009. The approach separated the carbonaceous  
733 aerosol into a natural and an anthropogenic fraction, and divided the anthropogenic fraction into fossil  
734 fuel and biomass burning origin, which is a prerequisite for targeted abatement strategies. The fraction  
735 apportioned to biomass burning was compared with calculated concentrations using the EMEP model,  
736 applying a base-case and an alternative emission set up with intermediate volatility compounds  
737 (IVOC).

738 The total carbonaceous aerosol concentration, as well as the carbonaceous aerosol apportioned  
739 to biomass burning, fossil fuel and natural sources, decreased from South to North. Natural sources  
740 typically accounted for a larger fraction of the carbonaceous aerosol in fall compared to winter/spring,  
741 likely because the fall sampling period partly took place in the vegetative season. The seasonal  
742 differences of the natural sources varied from minor at most sites, moderate at two of the continental  
743 sites, to substantial at the northernmost Scandinavian site. Biomass burning aerosol had an opposite  
744 seasonal behavior to that of natural sources, following the increased emissions from residential wood  
745 burning in the heating season. No consistent seasonal pattern was observed for fossil fuel aerosol and  
746 their contribution to the carbonaceous aerosol, possibly because domestic heating is a minor source of  
747 fossil fuel carbon compared to e.g. vehicular traffic.

748 Anthropogenic sources (60–78%) dominated at all but the most remote site in winter/spring,  
749 and residential wood burning (36–56%) was typically the major anthropogenic source of TC. In fall,  
750 anthropogenic and natural influence were of comparable magnitude at most sites, except at Birkenes  
751 (69% natural) and Ispra (77% anthropogenic). Biomass burning was the major anthropogenic source at  
752 Central European sites in fall (29–44%), whereas fossil fuel dominated at the southernmost (40%) and  
753 the three northernmost sites (29–37%).

754 Model calculated concentrations of carbonaceous aerosol from biomass burning were severely  
755 underestimated, except for the Scandinavian sites, when using the base-case MACC-III emission  
756 inventory. Model results improved when an alternative bottom-up approach with added IVOC was  
757 used. However, OC<sub>bb</sub> and EC<sub>bb</sub> levels were still substantially underestimated at the southernmost sites.

758 The current study shows that natural sources are major contributors to the carbonaceous  
759 aerosol at background sites in Europe even in fall and in winter/spring, and that residential wood  
760 burning emissions can be equally large or larger than that of fossil fuel sources, depending on season  
761 and region. Although the results of this particular study are for two relatively short periods, the general  
762 conclusions are consistent with those from multiple studies, which have pointed out the problems with  
763 European RWC inventories for both OC and EC (Simpson et al., 2007, Genberg et al., 2011, 2013,  
764 Bergström et al., 2012, Denier van der Gon, 2015a). The conclusions of the current study complement  
765 and reinforce these earlier results. Our combined results suggest that residential wood burning  
766 emissions are poorly constrained for large parts of Europe and that the need to improve emission  
767 inventories is obvious, with harmonized emission factors between countries likely being the most  
768 important step to improve model calculations. Revised wood burning emissions will also improve  
769 model predictions of PM<sub>2.5</sub> concentrations in Europe, particularly in the heating season. EMEP

770 intensive measurement periods are essential for real-world evaluation of model results, especially when  
771 the underlying emission data are so uncertain; as is future EMEP intensive measurement periods  
772 targeted on the wood burning source.

773

774 *Author Contributions.* KEY was responsible for the main design, coordination of the study, the  
775 synthesis of the results, writing most of the paper, responsible for the centralized analysis of  
776 levoglucosan, and provide OC/EC data for Birkenes. DS did the Latin Hybercube Sampling (LHS), as  
777 well as the EMEP modelling part together with RB. DS wrote the text on LHS, whereas DS and RB  
778 together wrote the text on the modelling, as well as they thoroughly reviewed the paper. GK wrote the  
779 introduction, provided OC/EC data for K-puszta and wrote the description of the site, and thoroughly  
780 reviewed the paper. SS and Y-LZ were responsible for and performed the centralized <sup>14</sup>C-analysis,  
781 wrote the text on this topic, and thoroughly reviewed the paper. WAA and ASHP contributed to the  
782 coordination of the study and thoroughly reviewed the paper. CH provided OC/EC data for Payerne,  
783 wrote the description of the site and thoroughly reviewed the paper. CP provided OC/EC data for  
784 Montelibretti, wrote the description of the site and thoroughly reviewed the paper. DC provided OC/EC  
785 data for Mace Head, wrote the description of the site and thoroughly reviewed the paper. GS provided  
786 OC/EC data for Melpitz, wrote the description of the site and thoroughly reviewed the paper. JPP  
787 provided OC/EC data for Ispra, wrote the description of the site and thoroughly reviewed the paper.  
788 JKN provided OC/EC data for Lille Valby and wrote the description of the site. MV provided OC/EC  
789 data for Košetice and wrote the description of the site. SE and IP thoroughly reviewed the paper.

790

791 *Competing interests.* The authors have no conflict of interest.

792

793 *Acknowledgements.* This work was supported by the Co-operative Programme for Monitoring and  
794 Evaluation of the Long-range Transmission of Air pollutants in Europe (EMEP) under UNECE, the  
795 European Union Seventh Framework Programme (FP7/2007–2013) under the ACTRIS project (Grant  
796 agreement #262254), and the European Union Seventh Framework Programme (FP7/2007–2013)  
797 under the ECLIPSE project Grant agreement #282688 – ECLIPSE. Computer time for EMEP model  
798 runs was supported by the Research Council of Norway through the NOTUR project EMEP  
799 (NN2890K), and this work was also supported by the Swedish Strategic Research Project MERGE  
800 (www.merge.lund.se). We are grateful to the Laboratory of Ion Beam Physics of ETH Zurich for  
801 providing the accelerator mass spectrometer MICADAS for <sup>14</sup>C measurements. We thank ECMWF and  
802 met.no for granting access to ECMWF analysis data. Hugo Denier van der Gon and Jeroen Kuenen  
803 from TNO are acknowledged for useful discussions and data concerning OM emissions.

804

805 **APPENDIX A**

806 **Detailed description of measurement sites**

807 The Montelibretti EMEP station is situated in central Italy (42°06'N, 12°38'E, 48 m asl) 45 km  
808 from the coast of the Tyrrhenian sea. Most of the land surrounding the station are meadows and low  
809 intensity agricultural areas. The nearest village (Monterotondo, 30 000 inhabitants) is situated  
810 approximately 5 km from the station, whereas the City of Rome lies 20 km to the south-west. Transport  
811 of air masses from the urban area of Rome is typically associated with sea-breeze taking place in the  
812 early afternoon.

813 The Ispra station (45° 49'N, 8° 38'E, 209 m asl) is situated on the edge of the Po Valley in the  
814 north-western part of Italy and is representative for the regional background of this densely populated  
815 part of Italy. Major anthropogenic emission sources are situated > 10 km from the site, with the city of  
816 Milan, 60 km to the south-east, as the most pronounced one. According to Henne et al. (2010), Ispra is  
817 categorized as a typical background site in an environment generally strongly affected by  
818 anthropogenic emissions.

819 The Payerne measurement station (46°48'N, 6°56'E, 489 m asl) is part of the Swiss national air  
820 pollution monitoring network as well as the EMEP monitoring network, and is regarded as a rural site.  
821 The station is located one kilometre south-east of the small town of Payerne (8 000 inhabitants). The  
822 site is surrounded by agricultural land (grassland and crops), forests and small villages. The nearest  
823 larger cities are Fribourg (15 km east, 35 000 inhabitants), Bern (40 km north east, 125 000 inhabitants)  
824 and Lausanne (40 km south-west, 120 000 inhabitants).

825 The K-pusztá station (46°58'N, 19°33'E, 130 m asl) is situated in a forest clearing on the  
826 Great Hungarian Plain and is representative for the Central-Eastern European regional background  
827 environment. The vegetation is dominated by coniferous wood (60%), but also deciduous wood (30%)  
828 and grassland are present. The nearest city (Kecskemét) is situated ca 15 km to the SE of K-pusztá. The  
829 station is part of the Global Atmospheric Watch (GAW) network, the European Monitoring and  
830 Evaluation Programme (EMEP) and is also a EUSAAR supersite. The climate is typically continental  
831 with low temperatures in winter, mild in spring and fall, and hot and sunny in summer.

832 The Košetice observatory (49°35'N, 15°05'E, 534 m asl) is a joint EMEP and GAW site  
833 located in the Czech-Moravian Highlands, approximately 80 km southeast from Prague. Air samples  
834 collected at the observatory represents the background level of air quality in the Czech Republic.  
835 Forests dominated by conifer trees account for approximately 50% of the land use in the vicinity of the  
836 site; the remaining 50% is attributed to meadow (25%) and agricultural areas (25%). The nearest city  
837 (Pelhřimov, 15 000 inhabitants) is located 25 km south of the station. The prevailing wind direction is  
838 westerly.

839 The Melpitz research station (51°32' N, 12°54' E, 87 m asl) is located on a flat meadow  
840 surrounded by agricultural land near the river Elbe. The major city Leipzig is situated 41 km to the  
841 south west of the site. Forested areas are located no closer than 1 km from the site. The two dominating  
842 wind directions are south west to west, which brings air masses from the Atlantic that passes across  
843 Western Europe, and east to south-east, which brings air masses from source regions such as Poland,  
844 Belarus, Ukraine and the north of the Czech Republic.

845           The Mace Head atmospheric research station (53°19'N, 9°53'W, 15 m asl) is a GAW supersite  
846 situated on the west coast of Ireland, facing the North Atlantic Ocean. The station is located 100 m  
847 from the coastline and is surrounded by bare land (rocks, grass and peat bog). A few scattered single  
848 houses are located at a distance of 1 km or further away. The nearest city (Galway, 80 000 inhabitants)  
849 is located 60 km to the east/south-east of the station. The site experience clean marine air masses from  
850 the western sector nearly 50% of the time, whereas polluted air masses are associated with atmospheric  
851 transport from UK and continental Europe.

852           Lille Valby (55°41' N, 12°07' E, 12 m asl) is a semi-rural monitoring station in the Sjælland  
853 region of Denmark, which has a humid continental climate. The surrounding area is characterized by  
854 agricultural land, small villages and the Roskilde Fjord (1 km west of the monitoring site). The station  
855 is located 30 km to the west of Copenhagen (1.2 million inhabitants), and 7 km North-East of central  
856 Roskilde (46 000 inhabitants). The nearest major road (A6) is located about 800 m west of the station.

857           The Birkenes atmospheric research station (58°23'N, 8°15'E, 190 m asl) is a joint supersite  
858 for EMEP and GAW situated approximately 20 km from the Skagerrak coast in southern Norway. The  
859 station is located in the boreal forest with mixed conifer and deciduous trees accounting for 65% of the  
860 land use in the vicinity of the site; the remaining 35% is attributed to meadow (10%), low intensity  
861 agricultural areas (10%), and freshwater lakes (15%). The nearest city (Kristiansand, 65 000  
862 inhabitants) is located 25 km south/south-west of the station, and is known to have minor or even  
863 negligible influence on the air quality at the site.

864

865 **References**

- 866 Andersson-Sköld, Y. & Simpson, D., Secondary organic aerosol formation in Northern Europe: a  
867 model study, *J. Geophys. Res.*, 2001, 106, 7357-7374.
- 868
- 869 Aas, W., Tsyro, S., Bieber, E., Bergström, R., Ceburnis, D., Ellermann, T., Fagerli, H., Frölich, M.,  
870 Gehrig, R., Makkonen, U., Nemitz, E., Otjes, R., Perez, N., Perrino, C., Prévôt, A. S. H., Putaud, J.-P.,  
871 Simpson, D., Spindler, G., Vana, M., and Yttri, K. E.: Lessons learnt from the first EMEP intensive  
872 measurement periods, *Atmos. Chem. Phys.*, 12, 8073-8094, doi:10.5194/acp-12-8073-2012, 2012.
- 873
- 874 Andreae, M. O. and Ramanathan, V.: Climate's dark forcings, *Science*, 340, 280–281, 2013.
- 875
- 876 Bauer, H., Schueller, E., Weinke, G., Berger, A., Hitzenberger, R., Marr, I. L., and Puxbaum, H.:  
877 Significant contributions of fungal spores to the organic carbon and to the aerosol mass balance of the  
878 urban atmospheric aerosol, *Atmos. Environ.*, 42, 5542–5549, 2008.
- 879
- 880 Bell, M. L., Ebisu, K., Peng, R. D., Samet, J. M., and Dominici, F.: Hospital Admissions and Chemical  
881 Composition of Fine Particle Air Pollution, *Am. J. Resp. Crit. Care*, 179, 1115–1120,  
882 doi:10.1164/rccm.200808-1240OC, 2009.
- 883
- 884 Bergström, R., Denier van der Gon, H. A. C., Prévôt, A. S. H., Yttri, K. E., and Simpson, D.:  
885 Modelling of organic aerosols over Europe (2002–2007) using a volatility basis set (VBS) framework:  
886 application of different assumptions regarding the formation of secondary organic aerosol, *Atmos.*  
887 *Chem. Phys.*, 12, 8499-8527, doi:10.5194/acp-12-8499-2012, 2012.
- 888
- 889 Bergström, R., Hallquist, M., Simpson, D., Wildt, J., and Mentel, T. F.: Biotic stress: a significant  
890 contributor to organic aerosol in Europe? *Atmos. Chem. Phys.*, 14, 13643-13660, 2014.
- 891
- 892 Bessagnet, B.; Menut, L.; Curci, G.; Hodzic, A.; Guillaume, B.; Liousse, C.; Moukhtar, S.; Pun, B.;  
893 Seigneur, C. & Schulz, M. Regional modeling of carbonaceous aerosols over Europe-focus on  
894 secondary organic aerosols *J. Atmos. Chem.*, 61, 175-202, 2008.
- 895
- 896 Birch, M. E. and Cary, R. A.: Elemental carbon-based method for monitoring occupational exposures  
897 to particulate diesel exhaust, *Aerosol Sci. Tech.*, 25, 221-241, 1996.
- 898
- 899 Bond, T. C., D. G. Streets, K. F. Yarber, S. M. Nelson, J.-H. Woo, and Z. Klimont. A technology-based  
900 global inventory of black and organic carbon emissions from combustion, *J. Geophys. Res.*, 109,  
901 D14203, doi:10.1029/2003JD003697, 2004.
- 902
- 903 Bond, T. C., Doherty, S. J., Fahey, D. W., Forster, P. M., Berntsen, T., DeAngelo, B. J., Flanner, M. G.,  
904 Ghan, S., Kärcher, B., Koch, D., Kinne, S., Kondo, Y., Quinn, P. K., Sarofim, M. C., Schultz, M. G.,  
905 Schulz, M., Venkataraman, C., Zhang, H., Zhang, S., Bellouin, N., Guttikunda, S. K., Hopke, P. K.,  
906 Jacobson, M. Z., Kaiser, J. W., Klimont, Z., Lohmann, U., Schwarz, J. P., Shindell, D., Storelvmo, T.,  
907 Warren, S. G., and Zender, C. S.: Bounding the role of black carbon in the climate system: a scientific  
908 assessment, *J. Geophys. Res. Atmos.*, 118, 5380-5552, 2013.



909

910 Bozzetti, C., Daellenbach, K. R., Hueglin, C., Fermo, P., Sciare, J., Kasper-Giebl, A., Mazar, Y.,  
911 Abbaszade, G., El Kazzi, M., Gonzalez, R., Shuster-Meiseles, T., Flasch, M., Wolf, R., Křepelová, A.,  
912 Canonaco, F., Schnelle-Kreis, J., Slowik, J. G., Zimmermann, R., Rudich, Y., Baltensperger, U., El  
913 Haddad, I., and Prévôt, A. S. H.: Size-resolved identification, characterization, and quantification of  
914 primary biological organic aerosol at a European rural site, *Environ. Sci. Technol.*, 50, 3425–3434,  
915 2016.

916

917 Buchholz, B. A., Fallon, S. J., Zermeno, P., Bench, G., and Schichtel, B. A.: Anomalous elevated  
918 radiocarbon measurements of PM<sub>2.5</sub>, *Nucl. Instrum. Methods Phys. Res. B*, 294, 631–635,  
919 doi:10.1016/j.nimb.2012.05.021, 2013.

920

921 Cassee, Flemming R., Heroux, M.-E., Gerlofs-Nijland, M. E., and Kelly, F. J.: Particulate matter  
922 beyond mass: recent health evidence on the role of fractions, chemical constituents and sources of  
923 emission, *Inhal Toxicol.*, 14, 802-12, doi:10.3109/08958378.2013.850127, 2013.

924

925 Ceburnis, D., Garbaras, A., Szidat, S., Rinaldi, M., Fahrni, S., Perron, N., Wacker, L., Leinert, S.,  
926 Remeikis, V., Facchini, M. C., Prevot, A. S. H., Jennings, S. G., Ramonet, M., and O'Dowd, C. D.:  
927 Quantification of the carbonaceous matter origin in submicron marine aerosol by <sup>13</sup>C and <sup>14</sup>C isotope  
928 analysis, *Atmos. Chem. Phys.*, 11, 8593-8606, doi:10.5194/acp-11-8593-2011, 2011.

929

930 Ciarelli, G., El Haddad, I., Bruns, E., Aksoyoglu, S., Möhler, O., Baltensperger, U., and Prévôt, A. S.  
931 H.: Constraining a hybrid volatility basis-set model for aging of wood-burning emissions using smog  
932 chamber experiments: a box-model study based on the VBS scheme of the CAMx model (v5.40),  
933 *Geosci. Model Dev.*, 10, 2303-2320, 2017.

934

935 Crippa, M., Canonaco, F., Lanz, V. A., Äijälä, M., Allan, J. D., Carbone, S., Capes, G., Ceburnis, D.,  
936 Dall'Osto, M., Day, D. A., DeCarlo, P. F., Ehn, M., Eriksson, A., Freney, E., Hildebrandt Ruiz, L.,  
937 Hillamo, R., Jimenez, J. L., Junninen, H., Kiendler-Scharr, A., Kortelainen, A.-M., Kulmala, M.,  
938 Laaksonen, A., Mensah, A. A., Mohr, C., Nemitz, E., O'Dowd, C., Ovadnevaite, J., Pandis, S. N.,  
939 Petäjä, T., Poulain, L., Saarikoski, S., Sellegri, K., Swietlicki, E., Tiitta, P., Worsnop, D. R.,  
940 Baltensperger, U., and Prévôt, A. S. H.: Organic aerosol components derived from 25 AMS data sets  
941 across Europe using a consistent ME-2 based source apportionment approach, *Atmos. Chem. Phys.*, 14,  
942 6159–6176, <https://doi.org/10.5194/acp-14-6159-2014>, 2014.

943

944 Crutzen, P. J. and Andreae, M. O.: Biomass burning in the tropics: impact on atmospheric chemistry  
945 and biogeochemical cycles, *Science*, 250, 1669-1678, 1990.

946

947 Denier van der Gon, H. A. C., Bergström, R., Fountoukis, C., Johansson, C., Pandis, S. N., Simpson,  
948 D., and Visschedijk, A. J. H.: Particulate emissions from residential wood combustion in Europe –

949 revised estimates and an evaluation, *Atmos. Chem. Phys.*, 15, 6503-6519, doi:10.5194/acp-15-6503-  
950 2015, 2015a.

951

952 Denier van der Gon, H. A. C., Kuenen, J. J. P., and Visschedijk, A. J. H.: Personal communication,  
953 2015b.

954

955 Diapouli, E., Popovicheva, O., Kistler, M., Vratolis, S., Persiantseva, N., Timofeev M., Kasper-Giebl,  
956 A., and Eleftheriadis, K.: Physicochemical characterization of aged biomass burning aerosol after long-  
957 range transport to Greece from large scale wildfires in Russia and surrounding regions, Summer 2010,  
958 *Atmos. Environ.*, 96, 393-404, 2014.

959

960 Dore, A. J., Carslaw, D. C., Braban, C., Cain, M., Chemel, C., Conolly, C., Derwent, R. G., Griffiths,  
961 S. J., Hall, J., Hayman, G., Lawrence, S., Metcalfe, S. E., Redington, A., Simpson, D., Sutton, M. A.,  
962 Sutton, P., Tang, Y. S., Vieno, M., Werner, M., Whyatt, J. D.: Evaluation of the performance of  
963 different atmospheric chemical transport models and inter-comparison of nitrogen and sulphur  
964 deposition estimates for the UK, *Atmos. Environ.*, 119, 131–143, 2015.

965

966 Dye, C. and Yttri, K. E.: Determination of monosaccharide anhydrides in atmospheric aerosols by use  
967 of high-resolution mass spectrometry combined with high performance liquid chromatography, *Anal.*  
968 *Chem.*, 77, 1853-1858, 2005.

969

970 Elsasser, M., Crippa, M., Orasche, J., DeCarlo, P. F., Oster, M., Pitz, M., Cyrus, J., Gustafson, T. L.,  
971 Pettersson, J. B. C., Schnelle-Kreis, J., Prevot, A. S. H., and Zimmermann, R.: Organic molecular  
972 markers and signature from wood combustion particles in winter ambient aerosols: aerosol mass  
973 spectrometer (AMS) and high time-resolved GC-MS measurements in Augsburg, Germany, *Atmos.*  
974 *Chem. Physics*, 12, 6113-6128, 2012.

975

976 Fahrni, S. M., Gäggeler, H. W., Hajdas, I., Ruff, M., Szidat, S., and Wacker, L.: Direct measurements  
977 of small <sup>14</sup>C samples after oxidation in quartz tubes, *Nucl. Instrum. Meth. Phys. Res. B.*, 268, 787-789,  
978 doi:10.1016/j.nimb.2009.10.031, 2010.

979

980 Fiore, A., Dentener, F., Wild, O., Cuvelier, C., Schultz, M., Textor, C., Schulz, M., Atherton, C.,  
981 Bergmann, D., Bey, I., Carmichael, G., Doherty, R., Duncan, B., Faluvegi, G., Folberth, G., Garcia  
982 Vivanco, M., Gauss, M., Gong, S., Hauglustaine, D., Hess, P., Holloway, T., Horowitz, L., Isaksen, I.,  
983 Jacob, D., Jonson, J., Kaminski, J., Keating, T., Lupu, A., MacKenzie, I., Marmer, E., Montanaro, V.,  
984 Park, R., Pringle, K., Pyle, J., Sanderson, M., Schroeder, S., Shindell, D., Stevenson, D., Szopa, S., Van  
985 Dingenen, R., Wind, P., Wojcik, G., Wu, S., Zeng, G. & Zuber, A.: Multi-model estimates of  
986 intercontinental source-receptor relationships for ozone pollution, *J. Geophys. Res.*, 2009, 114.

987

988 Forster, C., Wandering, U., Wotawa, G., James, P., Mattis, I., Althausen, D., Simmonds, P., O'Doherty,  
989 S., Jennings, S. G., Kleefeld, C., Schneider, J., Trickl, T., Kreipl, S., Jager, H. and Stohl, A.: Transport  
990 of boreal forest fire emissions from Canada to Europe, *J. Geophys. Res.*, 2001, 106, 22887-22906.  
991

992 Fuller, G. W., Tremper, A. H., Baker, T. D., Yttri, K. E., and Butterfield, D.: Contribution of wood  
993 burning to PM<sub>10</sub> in London, *Atmos. Environ.*, 87, 87-94. doi:10.1016/j.atmosenv.2013.12.037, 2014.  
994

995 Gelencsér, A.: Carbonaceous Aerosol, Atmospheric and Oceanographic Science Library Series, vol.  
996 30, Springer, New York, 2004.  
997

998 Gelencsér, A., May, B., Simpson, D., Sánchez-Ochoa, A., Kasper-Giebl, A., Puxbaum, H., Caseiro, A.,  
999 Pio, C., and Legrand, M.: Source apportionment of PM<sub>2.5</sub> organic aerosol over Europe:  
1000 primary/secondary, natural/anthropogenic, fossil/biogenic origin, *J. Geophys. Res.*, 112, D23S04, doi:  
1001 10.1029/2006JD008094, 2007.  
1002

1003 Genberg, J., Hyder, M., Stenström, K., Bergström, R., Simpson, D., Fors, E. O., Jönsson, J. Å., and  
1004 Swietlicki, E.: Source apportionment of carbonaceous aerosol in southern Sweden, *Atmos. Chem.*  
1005 *Phys.*, 11, 11387–11400, <https://doi.org/10.5194/acp-11-11387-2011>, 2011.  
1006

1007 Genberg, J., Denier van der Gon, H. A. C., Simpson, D., Swietlicki, E., Areskou, H., Beddows, D.,  
1008 Ceburnis, D., Fiebig, M., Hansson, H. C., Harrison, R. M., Jennings, S. G., Saarikoski, S., Spindler, G.,  
1009 Visschedijk, A. J. H., Wiedensohler, A., Yttri, K. E., and Bergström, R.: Light-absorbing carbon in  
1010 Europe – measurement and modelling, with a focus on residential wood combustion emissions, *Atmos.*  
1011 *Chem. Phys.*, 13, 8719-8738, doi:10.5194/acp-13-8719-2013, 2013.  
1012

1013 Gianini, M. F. D., Fischer, A., Gehrig, R., Ulrich, A., Wichser, A., Piot, C., Besombes, J.-L., and  
1014 Hueglin, C.: Sources of PM<sub>10</sub> in Switzerland: an analysis for 2008/2009 and changes since 1998/1999,  
1015 *Atmos. Environ.*, 54, 149-158, 2012.  
1016

1017 Gilardoni, S., Vignati, E., Cavalli, F., Putaud, J. P., Larsen, B. R., Karl, M., Stenström, K., Genberg, J.,  
1018 Henne, S., and Dentener, F.: Better constraints on sources of carbonaceous aerosols using a combined  
1019 14C - macro tracer analysis in a European rural background site, *Atmos. Chem. Physics*, 11, 5685-  
1020 5700, doi:10.5194/acp-11-5685-2011, 2011.  
1021

1022 Glasius, M., Hansen, A. M. K., Claeys, M., Henzing, J. S., Jedynska, A. D., Kasper-Giebl, A., Kistler,  
1023 M., Kristensen, K., Martinsson, J., Maenhaut, W., Nøjgaard, J. K., Spindler, G., Stenström, K. E.,  
1024 Swietlicki, E., Szidat, S., Simpson, D., and Yttri, K. E.: Composition and sources of carbonaceous  
1025 aerosols in Northern Europe during winter, *Atmos. Environ.*, 173, 127-141,  
1026 doi:10.1016/j.atmosenv.2017.11.005, 2018.  
1027

1028 Grieshop, A. P., Logue, J. M., Donahue, N. M., and Robinson, A. L.: Laboratory investigation of  
1029 photochemical oxidation of organic aerosol from wood fires 1: measurement and simulation of organic  
1030 aerosol evolution, *Atmos. Chem. Physics*, 9, 1263-1277, 2009.

1031

1032 Hallquist, M., Wenger, J. C., Baltensperger, U., Rudich, Y., Simpson, D., Claeys, M., Dommen, J.,  
1033 Donahue, N. M., George, C., Goldstein, A. H., Hamilton, J. F., Herrmann, H., Hoffmann, T., Iinuma,  
1034 Y., Jang, M., Jenkin, M. E., Jimenez, J. L., Kiendler-Scharr, A., Maenhaut, W., McFiggans, G., Mentel,  
1035 T. F., Monod, A., Prevot, A. S. H., Seinfeld, J. H., Surratt, J. D., Szmigielski, R., and Wildt, J.: The  
1036 formation, properties and impact of secondary organic aerosol: current and emerging issues,  
1037 *Atmospheric Chemistry and Physics*, 9, 5155-5236, 10.5194/acp-9-5155-2009, 2009.

1038

1039 Hao, W.M., Petkov, A., Nordgren, B.R., Corley, R.E., Silverstein, R.P., Urbanski, S.P., Evangeliou, N.,  
1040 Balkanski, Y., and Kinder, B.L. Daily black carbon emissions from fires in northern Eurasia for 2002–  
1041 2015. *Geosci. Model Dev.*, 9, 4461–4474. [www.geosci-model-dev.net/9/4461/2016/doi:10.5194/gmd-](http://www.geosci-model-dev.net/9/4461/2016/doi:10.5194/gmd-9-4461-2016)  
1042 [9-4461-2016](http://www.geosci-model-dev.net/9/4461/2016/doi:10.5194/gmd-9-4461-2016), 2016.

1043

1044 Heal, M. R., Naysmith, P., Cook, G. T., Xu, S., Duran, T. R., and Harrison, R. M.: Application of <sup>14</sup>C  
1045 analyses to source apportionment of carbonaceous PM<sub>2.5</sub> in the UK, *Atmos. Environ.*, 45, 2341-2348,  
1046 2011.

1047

1048 Henne, S., Brunner, D., Folini, D., Solberg, S., Klausen, J., and Buchmann, B.: Assessment of  
1049 parameters describing representativeness of air quality in-situ measurement sites, *Atmos. Chem. Phys.*,  
1050 10, 3561–3581, doi:10.5194/acp-10-3561-2010, 2010.

1051

1052 Herich, H., Gianini, M. F. D., Piot, C., Mocnik, G., Jaffrezo, J.-L., Besombes, J.-L., Prévôt, A. S. H.,  
1053 and Hueglin, C.: Overview of the impact of wood burning emissions on carbonaceous aerosols and PM  
1054 in large parts of the Alpine region, *Atmos. Environ.*, 89, 64-75, 2014.

1055

1056 Hodzic, A., Kasibhatla, P. S., Jo, D. S., Cappa, C. D., Jimenez, J. L., Madronich, S. and Park, R. J.:  
1057 Rethinking the global secondary organic aerosol (SOA) budget: stronger production, faster removal,  
1058 shorter lifetime, *Atmos. Chem. Physics*, 2016, 16, 7917-7941.

1059

1060 Jathar, S. H., Gordon, T. D., Hennigan, C. J., Pye, H. O. T., Pouliot, G., Adams, P. J., Donahue, N. M.,  
1061 and Robinson, A. L.: Unspeciated organic emissions from combustion sources and their influence on  
1062 the secondary organic aerosol budget in the United States, *Proc. Natl. Acad. Sci. Unit. States Am*, 111,  
1063 10473-10478, 2014.

1064

1065 Kanakidou, M., Seinfeld, J. H., Pandis, S. N., Barnes, I., Dentener, F. J., Facchini, M. C., Van  
1066 Dingenen, R., Ervens, B., Nenes, A., Nielsen, C. J., Swietlicki, E., Putaud, J. P., Balkanski, Y., Fuzzi,  
1067 S., Horth, J., Moortgat, G. K., Winterhalter, R., Myhre, C. E. L., Tsigaridis, K., Vignati, E., Stephanou,

1068 E. G., and Wilson, J.: Organic aerosol and global climate modelling: a review, *Atmos. Chem. Phys.*, 5,  
1069 1053–1123, doi:10.5194/acp-5-1053-2005, 2005.

1070

1071 Korontzi, S., McCarty, J., Loboda, T., Kumar, S., and Justice, C.: Global distribution of agricultural  
1072 fires in croplands from 3 years of Moderate Resolution Imaging Spectroradiometer (MODIS) data,  
1073 *Global Biogeochem. Cycles*, 20, GB2021, doi:10.1029/2005GB002529, 2006.

1074

1075 Kourtchev, I., Copolovici, L., Claeys, M., and Maenhaut, W.: Characterization of atmospheric aerosols  
1076 at a forested site in central Europe, *Environ. Sci. Technol.*, 43, 4665–4671, 2009.

1077

1078 Kristiansen, N. I., Stohl, A., and Wotawa, G.: Atmospheric removal times of the aerosol-bound  
1079 radionuclides <sup>137</sup>Cs and <sup>131</sup>I measured after the Fukushima Dai-ichi nuclear accident – a constraint for  
1080 air quality and climate models, *Atmos. Chem. Phys.*, 12, 10759–10769, 2012.

1081

1082 Kuenen, J. J. P., Visschedijk, A. J. H., Jozwicka, M., and Denier van der Gon, H. A. C.: TNO-  
1083 MACC\_II emission inventory; a multi-year (2003–2009) consistent high-resolution European emission  
1084 inventory for air quality modelling, *Atmos. Chem. Phys.*, 14, 10963-10976, doi:10.5194/acp-14-10963-  
1085 2014, 2014.

1086

1087 Kulmala, M., Asmi, A., Lappalainen, H. K., Carslaw, K. S., Pöschl, U., Baltensperger, U., Hov, Ø.,  
1088 Brenquier, J.-L., Pandis, S. N., Facchini, M. C., Hansson, H.-C., Wiedensohler, A., and O'Dowd, C.  
1089 D.: Introduction: European Integrated Project on Aerosol Cloud Climate and Air Quality interactions  
1090 (EUCAARI) – integrating aerosol research from nano to global scales, *Atmos. Chem. Phys.*, 9, 2825–  
1091 2841, doi:10.5194/acp-9-2825-2009, 2009.

1092

1093 Liu, J., Li, J., Vonwiller, M., Liu, D., Cheng, H., Shen, K., Salazar, G., Agrios, K., Zhang, Y., Hea, Q.,  
1094 Ding, X., Zhong, G., Wang, X., Szidat, S., and Zhang, G.: The importance of non-fossil sources in  
1095 carbonaceous aerosols in a megacity of central China during the 2013 winter haze episode: A source  
1096 apportionment constrained by radiocarbon and organic tracers, *Atmos. Environ.*, 144, 60-68,  
1097 doi:10.1016/j.atmosenv.2016.08.068, 2016.

1098

1099 López-Aparicio, S., Guevara, M., Thunis, P., Cuvelier, K. and Tarrasón, L.: Assessment of  
1100 discrepancies between bottom-up and regional emission inventories in Norwegian urban areas *Atmos.*  
1101 *Environ.*, 2017, 154, 285 – 296.

1102

1103 May, B., Wagenbach, D., Hammer, S., Steier, P., Puxbaum, H., and Pio, C.: The anthropogenic  
1104 influence on carbonaceous aerosol in the European background, *Tellus B*, 61, 464–472, 2009.

1105

1106 May, A. A., Levin, E. J. T., Hennigan, C. J., Riipinen, I., Lee, T., Collett Jr., J. L., Jimenez, J. L.,  
1107 Kreidenweis, S. M. and Robinson, A. L.: Gas-particle partitioning of primary organic aerosol

1108 emissions: 3. Biomass burning, *J. Geophys. Res. Atmos.*, 118, 11,327–11,338, doi:10.1002/jgrd.50828,  
1109 2013.  
1110  
1111 May, A. A., Levin, E. J. T., Hennigan, C. J., Riipinen, I., Lee, T., Collett Jr., J. L., Jimenez, J. L.,  
1112 Kreidenweis, S. M., and Robinson, A. L.: Gas-particle partitioning of primary organic aerosol  
1113 emissions: 3. Biomass burning, *J. Geophys. Res. Atmos.*, 118, 11,327–11,338, doi:10.1002/jgrd.50828,  
1114 2013a.  
1115  
1116 May, A. A., Presto, A. A., Hennigan, C. J., Nguyenm N. T., Gordon, T. D., and Robinson, A. L.: Gas-  
1117 Particle Partitioning of Primary Organic Aerosol Emissions: (2) Diesel Vehicles, *Environ. Sci.*  
1118 *Technol.*, 47, 8288–8296, doi:10.1021/es400782j, 2013b.  
1119  
1120 McDow, S. R. and Huntzicker, J. J.: Vapor adsorption artifact in the sampling of organic aerosol: face  
1121 velocity effects, *Atmos. Environ.*, 24, 2563–2571, 1990.  
1122  
1123 McFiggans, G., Mentel, T., Wildt, J., et al.: Secondary organic aerosol reduced by mixture of  
1124 atmospheric vapours, *Nature* 565, 587–593, 2019.  
1125  
1126 Mohn, J., Szidat, S., Fellner, J., Rechberger, H., Quartier, R., Buchmann, B., and Emmenegger, L.:  
1127 Determination of biogenic and fossil CO<sub>2</sub> emitted by waste incineration based on <sup>14</sup>CO<sub>2</sub> and mass  
1128 balances, *Bioresour. Technol.*, 99, 6471–6479, doi:10.1016/j.biortech.2007.11.042, 2008.  
1129  
1130 Novakov, T. and Penner, J.: Large contribution of organic aerosols to cloud condensation nuclei  
1131 concentrations, *Nature*, 365, 823–826, 1993.  
1132  
1133 O'Dowd, C., Ceburnis, D., Ovadnevaite, J., Vaishya, A., Rinaldi, M. and Facchini, M. C.: Do  
1134 anthropogenic, continental or coastal aerosol sources impact on a marine aerosol signature at Mace  
1135 Head?, *Atmos. Chem. Phys.*, 14, 10687–10704, <https://doi.org/10.5194/acp-14-10687-2014>, 2014.  
1136  
1137 Ots, R., Young, D. E., Vieno, M., Xu, L., Dunmore, R. E., Allan, J. D., Coe, H., Williams, L. R.,  
1138 Herndon, S. C., Ng, N. L., Hamilton, J. F., Bergström, R., Di Marco, C., Nemitz, E., Mackenzie, I. A.,  
1139 Kuenen, J. J. P., Green, D. C., Reis, S., and Heal, M. R.: Simulating secondary organic aerosol from  
1140 missing diesel-related intermediate-volatility organic compound emissions during the Clean Air for  
1141 London (ClearLo) campaign, *Atmos. Chem. Phys.*, 16, 6453–6473, [https://doi.org/10.5194/acp-16-](https://doi.org/10.5194/acp-16-6453-2016)  
1142 [6453-2016](https://doi.org/10.5194/acp-16-6453-2016), 2016.  
1143  
1144 Pope, C. A. and Dockery, D. W.: Health effects of fine particulate air pollution: lines that connect., *J.*  
1145 *Air Waste Manag. Assoc.*, 56, 709–742, 2006.  
1146

1147 Pöschl, U.: Aerosol particle analysis: challenges and progress, *Anal. Bioanal. Chem.*, 375, 30–32,  
1148 2003.  
1149  
1150 Pöschl, U.: Atmospheric aerosols: Composition, transformation, climate and health effects, *Angew.*  
1151 *Chem. Int. Ed.*, 44, 7520–7540. 2005.  
1152  
1153 Putaud, J.-P., R. Van Dingenen, A. Alastuey, H. Bauer, W. Birmili, J. Cyrys, H. Flentje, S. Fuzzi, R.  
1154 Gehrig, H.C. Hansson, R.M. Harrison, H. Hermann, R. Hitzenberger, C. Hüglin, A.M. Jones, A.  
1155 Kasper-Giebl, G. Kiss, A. Kousa, T.A.J. Kuhlbusch, G. Löschau, W. Maenhaut, A. Molnar, T. Moreno,  
1156 J. Pekkanen, C. Perrino, M. Pitz, H. Puxbaum, X. Querol, S. Rodriguez, I. Salma, J. Schwarz, J.  
1157 Smolik, J. Schneider, G. Spindler, H. ten Brink, J. Tursic, M. Viana, A. Wiedensohler and F. Raes: A  
1158 European Aerosol Phenomenology - 3: physical and chemical characteristics of particulate matter from  
1159 60 rural, urban, and kerbside sites across Europe, *Atmos. Environ.* 44, 1308-1320, 2010.  
1160  
1161 Puxbaum, H., Caseiro, A., Sánchez-Ochoa, A., Kasper-Giebl, A., Claeys, M., Gelencsér, A., Legrand,  
1162 M., Preunkert, S., Pio, C. A.: Levoglucosan levels at background sites in Europe for assessing the  
1163 impact of biomass combustion on the European, aerosol background, *J. Geophys. Res.*, 112, D23S05,  
1164 doi:10.1029/2006JD008114, 2007.  
1165  
1166 Querol, X., Alastuey, A., Pey, J., Cusack, M., P´erez, N., Mihalopoulos, N., Theodosi, C.,  
1167 Gerasopoulos, E., Kubilay, N., and Kocak, M.: Variability in regional background aerosols within the  
1168 Mediterranean, *Atmos. Chem. Phys.*, 9, 4575–4591, doi:10.5194/acp-9-4575-2009, 2009.  
1169  
1170 Reimer, P. J., Brown, T. A., and Reimer, R. W.: Discussion: Reporting and Calibration of PostBomb  
1171 <sup>14</sup>C Data, *Radiocarbon*, 46, 1299-1304, 2004.  
1172  
1173 Robinson, A. L., Donahue, N. M., Shrivastava, M. K., Weitkamp, E. A., Sage, A. M., Grieshop, A. P.,  
1174 Lane, T. E., Pierce, J. R., and Pandis, S. N.: Rethinking Organic Aerosols: Semivolatile Emissions and  
1175 Photochemical Aging, *Science*, 315, 1259-1262, 2007.  
1176  
1177 Rohr, A. C. and Wyzga, R. E.: Attributing health effects to individual particulate matter constituents,  
1178 *Atmos. Environ.*, 62, 130–152, doi:10.1016/j.atmosenv.2012.07.036, 2012.  
1179  
1180 Ruff, M., Wacker, L., Gäggeler, H. W., Suter, M., Synal, H. A., and Szidat, S.: A gas ion source for  
1181 radiocarbon measurements at 200 kV, *Radiocarbon*, 49, 307-314, 2007.  
1182  
1183 Simpson, D., Yttri, K. E., Klimont, Z., Kupiainen, K., Caseiro, A., Gelencsér, A., Pio, C., Legrand, M.:  
1184 Modeling carbonaceous aerosol over Europe. Analysis of the CARBOSOL and EMEP EC/OC  
1185 campaigns, *J. Geophys. Res.*, 112, D23S14, doi:10.1029/2006JD008114, 2007.  
1186

1187 Simpson, D., Benedictow, A., Berge, H., Bergström, R., Emberson, L. D., Fagerli, H., Flechard, C. R.,  
1188 Hayman, G. D., Gauss, M., Jonson, J. E., Jenkin, M. E., Nyíri, A., Richter, C., Semeena, V. S., Tsyro,  
1189 S., Tuovinen, J.-P., Valdebenito, Á., and Wind, P.: The EMEP MSC-W chemical transport model –  
1190 technical description, *Atmos. Chem. Phys.*, 12, 7825-7865, doi:10.5194/acp-12-7825-2012, 2012.

1191

1192 Simpson, D. and Denier van der Gon, H.: Problematic emissions - particles or gases? in:  
1193 Transboundary particulate matter, photo-oxidants, acidifying and eutrophying components, EMEP  
1194 Status Report 1/2015, The Norwegian Meteorological Institute, Oslo, Norway, 87-96, 2015.

1195

1196 Simpson, D., Bergström, R., Imhof, H., and Wind, P.: Updates to the EMEP/MSW model, 2016-  
1197 2017, in: Transboundary particulate matter, photo-oxidants, acidifying and eutrophying components,  
1198 Status Report 1/2017, The Norwegian Meteorological Institute, Oslo, Norway, 115-122, 2017.

1199

1200 Spindler, G., Gnauk, T., Grüner, A., Iinuma, Y., Müller, K., Scheinhardt, S. and Herrmann, H.: Size-  
1201 segregated characterization of PM<sub>10</sub> at the EMEP site Melpitz (Germany) using a five-stage impactor: a  
1202 six year study. *J. Atmos. Chem.*, 69, 127-157, 2012.

1203

1204 Stohl, A., Berg, T., Burkhardt, J. F., Fjæraa, A. M., Forster, C., Herber, A., Hov, Ø., Lunder, C.,  
1205 McMillan, W. W., Oltmans, S., Shiobara, M., Simpson, D., Solberg, S., Stebel, K., Ström, J., Tørseth,  
1206 K., Treffeisen, R., Virkkunen, K., and Yttri, K. E.: Arctic smoke - record high air pollution levels in the  
1207 European Arctic due to agricultural fires in Eastern Europe, *Atmos. Chem. Phys.*, 7, 511–534, 2007.

1208

1209 Subramanian, R., Khlystov, A. Y., and Robinson, A. L.: Effect of Peak Inert-Mode Temperature on  
1210 Elemental Carbon Measured Using Thermal-Optical Analysis, *Aerosol Science and Technology*, 40:10,  
1211 763–780, doi: 10.1080/02786820600714403, 2006.

1212

1213 Szidat, S., Jenk, T. M., Gäggeler, H. W., Synal, H. A., Fisseha, R., Baltensperger, U., Kalberer, M.,  
1214 Samburova, V., Reimann, S., Kasper-Giebl, A., and Hajdas, I.: Radiocarbon (<sup>14</sup>C)-deduced biogenic  
1215 and anthropogenic contributions to organic carbon (OC) of urban aerosols from Zurich, Switzerland,  
1216 *Atmos. Environ.*, 38, 4035–4044, 2004.

1217

1218 Szidat, S., Prevot, A. S. H., Sandradewi, J., Alfarra, M. R., Synal, H.-A., Wacker, L., Baltensperger, U.:  
1219 Dominant impact of residential wood burning on particulate matter in Alpine valleys during winter,  
1220 *Geophys. Res. Lett.*, 34, L05820, doi:10.1029/2006GL028325, 2007.

1221

1222 Szidat, S., Ruff, M., Perron, N., Wacker, L., Synal, H.-A., Hallquist, M., Shannigrahi, A. S., Yttri, K.  
1223 E., Dye, C., and Simpson, D.: Fossil and non-fossil sources of organic carbon (OC) and elemental  
1224 carbon (EC) in Göteborg, Sweden. *Atmos. Chem. Phys.* 9, 1521–1535, doi:10.5194/acp-9-1521-2009,  
1225 2009.

1226



1227 Tsyro, S., Simpson, D., Tarrasón, L., Kupiainen, K., Klimont, Z., Yttri, K. and Pio, C.: Modelling of  
1228 elemental carbon over Europe, *J. Geophys. Res.*, 112, D23S19, 2007.  
1229  
1230 Viana, M., Kuhlbusch, T. A., Querol, X., Alastuey, A., Harrison, R. M., Hopke, P. K., Winiwarter, W.,  
1231 Vallius, M., Szidat, S., Prevot, A. S. H., Hueglin, C., Bloemen, H., Wahlin, P., Vecchi, R., Miranda, A.  
1232 I., Kasper-Giebl, A., Maenhaut, W., Hitzenberger, R.: Source apportionment of particulate matter in  
1233 Europe: a review of methods and results, *J. Aerosol Sci.*, 39, 827-849,  
1234 doi:10.1016/j.jaerosci.2008.05.007, 2008.  
1235  
1236 Vieno, M., Heal, M. R., Williams, M. L., Carnell, E. J., Nemitz, E., Stedman, J. R., and Reis, S.: The  
1237 sensitivities of emissions reductions for the mitigation of UK PM<sub>2.5</sub>, *Atmos. Chem. Phys.*, 16, 265–276,  
1238 https://doi.org/10.5194/acp-16-265-2016, 2016.  
1239  
1240 Wacker, L., Fahrni, S. M., Hajdas, I., Molnar, M., Synal, H.-A., Szidat, S., and Zhang, Y.L.: A versatile  
1241 gas interface for routine radiocarbon analysis with a gas ion source, *Nucl. Instr. Meth. Phys. Res. B*,  
1242 294, 315-319, doi:10.1016/j.nimb.2012.02.009, 2013.  
1243  
1244 Wagener, S., Langner, M., Hansen, U., Moriske, H. J., Endlicher, W. R., and Wilfried, R.: Spatial and  
1245 seasonal variations of biogenic tracer compounds in ambient PM<sub>10</sub> and PM<sub>1</sub> samples in Berlin,  
1246 Germany, *Atmos. Environ.*, 47, 33-42, doi:10.1016/j.atmosenv.2011.11.044, 2012.  
1247  
1248 Waked, A., Favez, O., Alleman, L. Y., Piot, C., Petit, J.-E., Delaunay, T., Verlinden, E., Golly, B.,  
1249 Besombes, J.-L., Jaffrezo, J.-L., and Leoz-Garziandia, E.: Source apportionment of PM<sub>10</sub> in a north-  
1250 western Europe regional urban background site (Lens, France) using positive matrix factorization and  
1251 including primary biogenic emissions, *Atmos. Chem. Phys.*, 14, 3325–3346,  
1252 https://doi.org/10.5194/acp-14-3325-2014, 2014.  
1253  
1254 Wallén, A., Lidén, G., and Hansson H. C.: Measured Elemental Carbon by Thermo-Optical  
1255 Transmittance Analysis in Water-Soluble Extracts from Diesel Exhaust, Woodsmoke, and Ambient  
1256 Particulate Samples, *J. Occup. Environ. Med.*, 7, 35–41, doi: 10.1080/15459620903368859, 2010.  
1257  
1258 Wiedinmyer, C., Yokelson, R. J., and Gullett, B. K.: Global Emissions of Trace Gases, Particulate  
1259 Matter, and Hazardous Air Pollutants from Open Burning of Domestic Waste, *Environ. Sci. Technol.*,  
1260 48, 9523-9530, 2014.  
1261  
1262 Winiwarter, W., Bauer, H., Caseiro, A., and Puxbaum, H.: Quantifying emissions of primary biological  
1263 aerosol particle mass in Europe, *Atmos. Environ.*, 43, 1403-1409, 2009.  
1264

1265 Yang, H. and Yu, J. Z.: Uncertainties in Charring Correction in the Analysis of Elemental and Organic  
1266 Carbon in Atmospheric Particles by Thermal/Optical Methods, *Environ Sci Technol.*, 36,5199-5204,  
1267 2002.  
1268  
1269 Yttri, K. E., Aas, W., Bjerke, A., Cape, J. N., Cavalli, F., Ceburnis, D., Dye, C., Emblico, L., Facchini,  
1270 M. C., Forster, C., Hanssen, J. E., Hansson, H. C., Jennings, S. G., Maenhaut, W., Putaud, J. P.,  
1271 Tørseth, K.: Elemental and organic carbon in PM<sub>10</sub>: A one year measurement campaign within the  
1272 European monitoring and Evaluation Programme EMEP, *Atmos. Chem. Phys.*, 7, 5711-5725, 2007a.  
1273  
1274 Yttri, K. E., Dye, C., Kiss, G.: Ambient aerosol concentrations of sugars and sugar-alcohols at four  
1275 different sites in Norway, *Atmos. Chem. Phys.*, 7, 4267-4279, 2007b.  
1276  
1277 Yttri, K. E., Simpson, D., Stenström, K., Puxbaum, H., and Svendby, T.: Source apportionment of the  
1278 carbonaceous aerosol in Norway quantitative estimates based on <sup>14</sup>C, thermal-optical and organic tracer  
1279 analysis, *Atmos. Chem. Phys.*, 11, 9375–9394, doi:10.5194/acp-11-9375-2011, 2011a.  
1280  
1281 Yttri, K. E., Simpson, D., Nøjgaard, J. K., Kristensen, K., Genberg, J., Stenström, K., Swietlicki, E.,  
1282 Hillamo, R., Aurela, M., Bauer, H., Offenberg, J. H., Jaoui, M., Dye, C., Eckhardt, S., Burkhardt, J. F.,  
1283 Stohl, A., and Glasius, M.: Source apportionment of the summer time carbonaceous aerosol at Nordic  
1284 rural background sites, *Atmos. Chem. Phys.*, 11, 13339–13357, doi:10.5194/acp- 11-13339-2011,  
1285 2011b.  
1286  
1287 Yttri, K. E., Lund Myhre, C., Eckhardt, S., Fiebig, M., Dye, C., Hirdman, D., Ström, J., Klimont, Z.,  
1288 Stohl, A. (2014) Quantifying black carbon from biomass burning by means of levoglucosan – a one-  
1289 year time series at the Arctic observatory Zeppelin. *Atmos. Chem. Phys.*, 14, 6427-6442,  
1290 doi:10.5194/acp-14-6427-2014, 2014.  
1291  
1292 Yttri, K. E., Schnelle-Kreis, J., Maenhaut, W., Abbaszade, G., Alves, C., Bjerke, A., Bonnier, N.,  
1293 Bossi, R., Claeys, M., Dye, C., Evtyugina, M., García-Gacio, D., Hillamo, R., Hoffer, A., Hyder, M.,  
1294 Inuma, Y., Jaffrezo, J.-L., Kasper-Giebl, A., Kiss, G., López-Mahia, P. L., Pio, C., Piot, C., Ramirez-  
1295 Santa-Cruz, C., Sciare, J., Teinilä, K., Vermeylen, R., Vicente, A., Zimmermann, R. (2015) An  
1296 intercomparison study of analytical methods used for quantification of levoglucosan in ambient aerosol  
1297 filter samples, *Atmos. Meas. Tech.*, 8, 125-147, doi:10.5194/amt-8-125-2015, 2015.  
1298  
1299 Yttri et al. (*In prep.*)  
1300  
1301 Zappoli, S., Andracchio, A., Fuzzi, S., Facchini, M. C., Gelencsér, A., Kiss, G., Krivácsy, Z., Molnár,  
1302 Á., Mészáros, E., Hansson, H. -C., Rosman, K., and Zebühr, Y.: Inorganic, organic and  
1303 macromolecular components of fine aerosol in different areas of Europe in relation to their water  
1304 solubility, *Atmos. Environ.*, 33, 2733–2743, [https://doi.org/10.1016/S1352-2310\(98\)00362-8](https://doi.org/10.1016/S1352-2310(98)00362-8), 1999.

1305  
1306 Zhang, Q., Jimenez, J. L., Canagaratna, M. R., Allan, J. D., Coe, H., Ulbrich, I., Alfarra, M. R.,  
1307 Takami, A., Middlebrook, A. M., Sun, Y. L., Dzepina, K., Dunlea, E., Docherty, K., DeCarlo, P. F.,  
1308 Salcedo, D., Onasch, T., Jayne, J. T., Miyoshi, T., Shimojo, A., Hatakeyama, Takegawa, N., Kondo,  
1309 Y., Schneider, J., Drewnick, F., Borrmann, S., Weimer, S., Demerjian, K., Williams, P., Bower, K.,  
1310 Bahreini, R., Cottrell, L., Griffin, R. J., Rautiainen, J., Sun, J. Y., Zhang, Y. M., and Worsnop, D. R.:  
1311 Ubiquity and dominance of oxygenated species in organic aerosols in anthropogenically-influenced  
1312 Northern Hemisphere midlatitudes, *Geophys. Res. Lett.*, 34, L13801, doi:10.1029/2007GL029979,  
1313 2007.  
1314  
1315 Ziemann, PJ, Atkinson, R: Kinetics, products, and mechanisms of secondary organic aerosol formation,  
1316 *Chem. Soc. Rev.*, 41, 6582-6605, doi:10.1039/c2cs35122f, 2012.  
1317  
1318 Zotter, P., Ciobanu, V. G., Zhang, Y. L., El-Haddad, I., Macchia, M., Daellenbach, K. R., Salazar, G.  
1319 A., Huang, R.-J., Wacker, L., Hueglin, C., Piazzalunga, A., Fermo, P., Schwikowski, M.,  
1320 Baltensperger, U., Szidat, S., and Prévôt, A. S. H.: Radiocarbon analysis of elemental and organic  
1321 carbon in Switzerland during winter-smog episodes from 2008 to 2012 -- Part 1: Source apportionment  
1322 and spatial variability, *Atmos. Chem. Phys.*, 14, 13551-13570, 2014.

**Table 1: Location of the nine European rural background sites that participated in the Fall 2008 and Winter/spring 2009 sampling periods. The sites are ordered by latitude from south to north.**

Sampling site	Location	Height (m asl)	Sampling period	Cut-off size	Flow rate (l min <sup>-1</sup> )	Filter face velocity (cm s <sup>-1</sup> )	Ambient temp. (min-max)	Precip. (min-max)
Montelibretti (Italy)	42° 06'N, 12° 38'E	48	24.09–15.10.2008	PM <sub>10</sub>	38	54	16.8 (16.2-17.1)	0.8 (0-2.4)
			25.02–25.03.2009				9.9 (8.5-11)	16.6 (1.2-45.8)
Ispra (Italy)	45° 48'N, 08° 38'E	209	24.09–22.10.2008	PM <sub>10</sub>	16.7	20	13.0 (12.8-13.3)	NA
			25.02–25.03.2009				8.0 (7-9.6)	NA
Payerne (Switzerland)	46° 48'N, 06° 56'E	489	16.09–16.10.2008	PM <sub>10</sub>	16.7	23	10.5 (9.2-12.5)	1.4 (0.6-2.5)
			27.02–25.03.2009				4.4 (2.9-6.5)	1.4 (0-3.9)
K-pusztá (Hungary)	46°58'N, 19°33'E	130	17.09–15.10.2008	PM <sub>10</sub>	16.7	22	11.7 (9.9-12.6)	9.3 (0-19.4)
			25.02–25.03.2009				5.1 (3.7-7.2)	5.3 (1.3-10.5)
Košetice (Czech Rep.)	49°35'N, 15°05'E	534	17.09–15.10.2008	PM <sub>10</sub>	38	53	9.6 (7.5-11.9)	7.4 (2.7-16.6)
			25.02–25.03.2009				2.0 (0.4-3.4)	17.3 (11.3-23.2)
Melpitz (Germany)	51°32' N, 12°54'E	87	17.09–15.10.2008	PM <sub>10</sub>	16.7	22	11.2 (10.6-12.3)	7.6 (3.1-14.3)
			25.02–25.03.2009				5.4 (3.7-6.8)	13.2 (9.5-16.6)
Mace Head (Ireland)	53° 19'N, 09° 53'W	15	18.09–15.10.2008	PM <sub>2.5</sub>	1111	45	12.4 (11.3–12.9)	17.3 (0–51.2)
			25.02–25.03.2009				8.3 (7.1–9.4)	12.4 (0.1–37.1)
Lille Valby (Denmark)	55° 41'N, 12° 08'E	10	17.09–15.09.2008	PM <sub>10</sub>	38	56	10.9 (9.2-12)	7.6 (0.3-21.7)
			25.02–25.03.2009				5.2 (2.7-10.3)	9.7 (3.321.3)
Birkenes (Norway)	58° 23'N, 8° 15'E	190	17.09–15.10.2008	PM <sub>10</sub>	38	54	8.2 (6-9.4)	31.1 (7.6-53.1)
			25.02–25.03.2009				-0.7 (-1.5-0.3)	22.5 (0.2-48.5)

**Table 2a: Mean ( $\pm$  SD; standard deviation) concentrations of carbonaceous sub-fractions and levoglucosan in PM<sub>10</sub><sup>1</sup> during Winter/Spring 2009. The EC/TC<sub>p</sub> ratio, the OC<sub>Back</sub>/OC<sub>Front</sub> ratio and non-fossil fractions of TC<sub>p</sub> (f<sub>nf</sub>(TC<sub>p</sub>)) are also listed. The sites are ordered by latitude from south to north.**

	Montelibretti	Ispra	Payerne	K-pusztá	Košetice	Melpitz	Mace Head <sup>1</sup>	Lille Valby	Birkenes
<i>Unit: (<math>\mu\text{g C m}^{-3}</math>)</i>									
TC <sub>p</sub>	6.1 $\pm$ 2.7	9.3 $\pm$ 5.7	3.6 $\pm$ 1.3	5.5 $\pm$ 2.8	2.1 $\pm$ 0.78	1.7 $\pm$ 0.68	0.76 $\pm$ 0.91	1.5 $\pm$ 0.33	0.44 $\pm$ 0.13
OC <sub>p</sub>	5.0 $\pm$ 2.5	7.9 $\pm$ 5.0	2.9 $\pm$ 1.0	4.8 $\pm$ 2.6	1.8 $\pm$ 0.70	1.3 $\pm$ 0.50	0.65 $\pm$ 0.79	1.2 $\pm$ 0.3	0.34 $\pm$ 0.08
OC <sub>Back</sub>	0.62 $\pm$ 0.16	0.50 $\pm$ 0.22	0.41 $\pm$ 0.18	0.35 $\pm$ 0.10	0.23 $\pm$ 0.09	0.41 $\pm$ 0.26	0.07 $\pm$ 0.04	0.53 $\pm$ 0.31	0.13 $\pm$ 0.13
EC	1.0 $\pm$ 0.25	1.5 $\pm$ 0.68	0.66 $\pm$ 0.27	0.77 $\pm$ 0.21	0.32 $\pm$ 0.12	0.40 $\pm$ 0.12	0.11 $\pm$ 0.13	0.37 $\pm$ 0.09	0.10 $\pm$ 0.05
<i>Unit: (%)</i>									
EC/TC <sub>p</sub>	18 $\pm$ 3.6	17 $\pm$ 2.3	19 $\pm$ 2.9	15 $\pm$ 3.3	16 $\pm$ 1.4	24 $\pm$ 4.1	14 $\pm$ 1.3	24 $\pm$ 5.4	21 $\pm$ 5.2
OC <sub>Back</sub> /OC <sub>Front</sub>	12 $\pm$ 2.9	6.6 $\pm$ 1.3	12 $\pm$ 1.9	7.3 $\pm$ 1.4	12 $\pm$ 4.4	24 $\pm$ 12	23 $\pm$ 21	30 $\pm$ 10	24 $\pm$ 13
<i>Unit: (Fraction)</i>									
f <sub>nf</sub> (TC <sub>p</sub> )	0.80 $\pm$ 0.06	0.80 $\pm$ 0.05	0.90 $\pm$ 0.09	0.83 $\pm$ 0.09	0.69 $\pm$ 0.04	0.83 $\pm$ 0.13	0.79 $\pm$ 0.11	0.71 $\pm$ 0.13	0.77 $\pm$ 0.09
<i>Unit: (ng m<sup>-3</sup>)</i>									
Levoglucosan	247 $\pm$ 113	668 $\pm$ 295	141 $\pm$ 63	209 $\pm$ 156	67 $\pm$ 16	57 $\pm$ 20	12 $\pm$ 13	41 $\pm$ 5.5	17 $\pm$ 7.7

1) For Mace Head PM<sub>2.5</sub> was used

**Table 2b: Mean ( $\pm$  SD; standard deviation) concentrations of carbonaceous sub-fractions and levoglucosan in PM<sub>10</sub><sup>1</sup> during Fall 2008. The EC/TC<sub>p</sub> ratio, the OC<sub>Back</sub>/OC<sub>Front</sub> ratio and non-fossil fractions of TC<sub>p</sub> (f<sub>nf</sub>(TC<sub>p</sub>)) are also listed. The sites are ordered from by latitude south to north.**

	Montelibretti <sup>2</sup>	Ispira	Payerne	K-pusztá	Košetice	Melpitz	Mace Head <sup>1</sup>	Lille Valby	Birkenes
<i>Unit: (<math>\mu\text{g C m}^{-3}</math>)</i>									
TC <sub>p</sub>	5.0 $\pm$ 1.8	7.6 $\pm$ 2.5	3.9 $\pm$ 1.1	6.7 $\pm$ 2.9	3.3 $\pm$ 0.66	2.1 $\pm$ 0.36	0.89 $\pm$ 1.2	1.8 $\pm$ 0.74	1.1 $\pm$ 0.47
OC <sub>p</sub>	4.0 $\pm$ 1.8	6.1 $\pm$ 2.0	3.3 $\pm$ 0.93	5.5 $\pm$ 2.7	2.8 $\pm$ 0.59	1.6 $\pm$ 0.21	0.77 $\pm$ 1.1	1.3 $\pm$ 0.70	0.97 $\pm$ 0.45
OC <sub>Back</sub>	0.75 $\pm$ 0.16	0.47 $\pm$ 0.31	0.53 $\pm$ 0.37	0.33 $\pm$ 0.08	0.21 $\pm$ 0.08	0.60 $\pm$ 0.33	0.10 $\pm$ 0.07	0.48 $\pm$ 0.21	0.17 $\pm$ 0.03
EC	0.97 $\pm$ 0.25	1.5 $\pm$ 0.54	0.59 $\pm$ 0.17	1.2 $\pm$ 0.26	0.49 $\pm$ 0.10	0.54 $\pm$ 0.16	0.12 $\pm$ 0.17	0.46 $\pm$ 0.10	0.11 $\pm$ 0.03
<i>Unit: (%)</i>									
EC/TC <sub>p</sub>	21 $\pm$ 8.3	20 $\pm$ 3.7	15 $\pm$ 0.31	18 $\pm$ 4.0	15 $\pm$ 2.1	25 $\pm$ 3.7	12 $\pm$ 5.6	28 $\pm$ 8.1	11 $\pm$ 3.3
OC <sub>Back</sub> /OC <sub>Front</sub>	17 $\pm$ 3.8	6.8 $\pm$ 2.6	13 $\pm$ 4.9	5.9 $\pm$ 1.0	6.9 $\pm$ 1.5	26 $\pm$ 10	19 $\pm$ 8.9	28 $\pm$ 13	19 $\pm$ 6.7
<i>Unit: (Fraction)</i>									
f <sub>nf</sub> (TC <sub>p</sub> )	0.61 $\pm$ 0.01	0.69 $\pm$ 0.08	0.80 $\pm$ 0.06	0.81 $\pm$ 0.03	0.86 $\pm$ 0.10	0.76 $\pm$ 0.04	0.70 $\pm$ 0.18	0.72 $\pm$ 0.12	0.75 $\pm$ 0.05
<i>Unit: (<math>\text{ng m}^{-3}</math>)</i>									
Levoglucosan	106 $\pm$ 40	364 $\pm$ 180	85 $\pm$ 16	172 $\pm$ 84	83 $\pm$ 14	33 $\pm$ 14	16 $\pm$ 19	32 $\pm$ 19	6.8 $\pm$ 2.2

1) For Mace Head PM<sub>2.5</sub> was used.

2) The sampler at Montelibretti was run in an alternating on/off mode, collecting ambient air 15 minutes every 1 hour.

**Table 3: Volatility distributions of the primary organic aerosol (POA) emissions from anthropogenic sources.**

$C^*$ ( $\mu\text{g m}^{-3}$ ) <sup>a</sup>		$10^{-2}$	$10^{-1}$	1	10	$10^2$	$10^3$	$10^4$	$10^5$	$10^6$
<b>Base-case emission fraction<sup>b</sup></b>	SNAP 2	0.20	0.00	0.10	0.10	0.20	0.40	0.00	0.00	0.00
	all other sources	0.00	0.04	0.25	0.37	0.23	0.11	0.00	0.00	0.00
<b>DT+IVOC emission fraction<sup>c, d</sup></b>	SNAP 2	0.025	0.050	0.076	0.118	0.151	0.252	0.336	0.42	0.672
	all other sources	0.03	0.06	0.09	0.14	0.18	0.30	0.40	0.50	0.80

<sup>a</sup>  $C^*$ : Saturation concentration at 298 K; enthalpies of vaporization were taken from May et al. (2013a,b) for the base-case (MACC-III), and from Shrivastava et al. (2008) for the DT+IVOC case.

<sup>b</sup> The volatility distribution in the MACC-III model run is based on the recommended volatility distributions from May et al. (2013a,b) for biomass burning emissions (for SNAP sector 2; non-industrial stationary combustion) and for diesel exhaust (for all the other emission sectors), but moving the emissions in the  $C^*=10^4 \mu\text{g m}^{-3}$ – $10^6 \mu\text{g m}^{-3}$  bins to the  $10^3 \mu\text{g m}^{-3}$  bin.

<sup>c</sup> The volatility distributions in the DT+IVOC case are based on Shrivastava et al. (2008) for all emission sectors except SNAP-2, for which it is based on the distribution used for the EMEP model in Denier van der Gon et al. (2015a). Note that this scenario assumes that there are substantial IVOC emissions that are not included in the emission inventories (see Bergström et al., 2012, and Denier van der Gon et al., 2015a).

<sup>d</sup> Since the DT emission inventory by Denier van der Gon et al. (2015a) was constructed to include a larger fraction of SVOC from residential wood burning emissions, we apply a slightly different emission split for the SNAP-2 POA compared to other SNAP sectors. Considering both SVOC and IVOC within the POA class, the total POA emissions are assumed to be 2.1 times the inventory (compared to the factor 2.5 for the other emission sectors).

**Table 4: Model and source apportioned (LHS-derived) concentrations of elemental carbon (EC<sub>bb</sub>) and organic carbon (OC<sub>bb</sub>) from biomass burning. Model results are averages over both measurement periods (Fall 2008 and Winter/Spring 2009). For the LHS-results the mean of the 10- and 90-percentiles are shown. Unit:  $\mu\text{g C m}^{-3}$ .**

Site	EC <sub>bb</sub>				OC <sub>bb</sub>			
	Base-case	DT+IVOC	LHS-10	LHS-90	Base-case	DT+IVOC	LHS-10	LHS-90
Montelibretti	0.19	0.097	0.29	0.70	0.28	0.37	1.04	2.38
Ispra	0.34	0.21	0.47	0.93	0.63	0.82	1.70	3.16
K-pusztta	0.20	0.17	0.30	0.67	0.37	0.74	1.10	2.27
Payerne	0.081	0.24	0.20	0.46	0.12	0.79	0.73	1.51
Košetice	0.074	0.17	0.12	0.28	0.14	0.60	0.42	0.91
Melpitz	0.063	0.096	0.085	0.18	0.12	0.37	0.30	0.57
Mace Head	0.0045	0.0091	0.028	0.057	0.015	0.061	0.086	0.16
Lille Valby	0.24	0.18	0.067	0.14	0.22	0.36	0.24	0.46
Birkenes	0.065	0.047	0.020	0.046	0.13	0.17	0.072	0.15





**Figure 1: Overview of sampling sites participating in the carbonaceous aerosol source-apportionment study in the EMEP intensive measurement periods (IMPs) in Fall 2008 and Winter/spring 2009.**

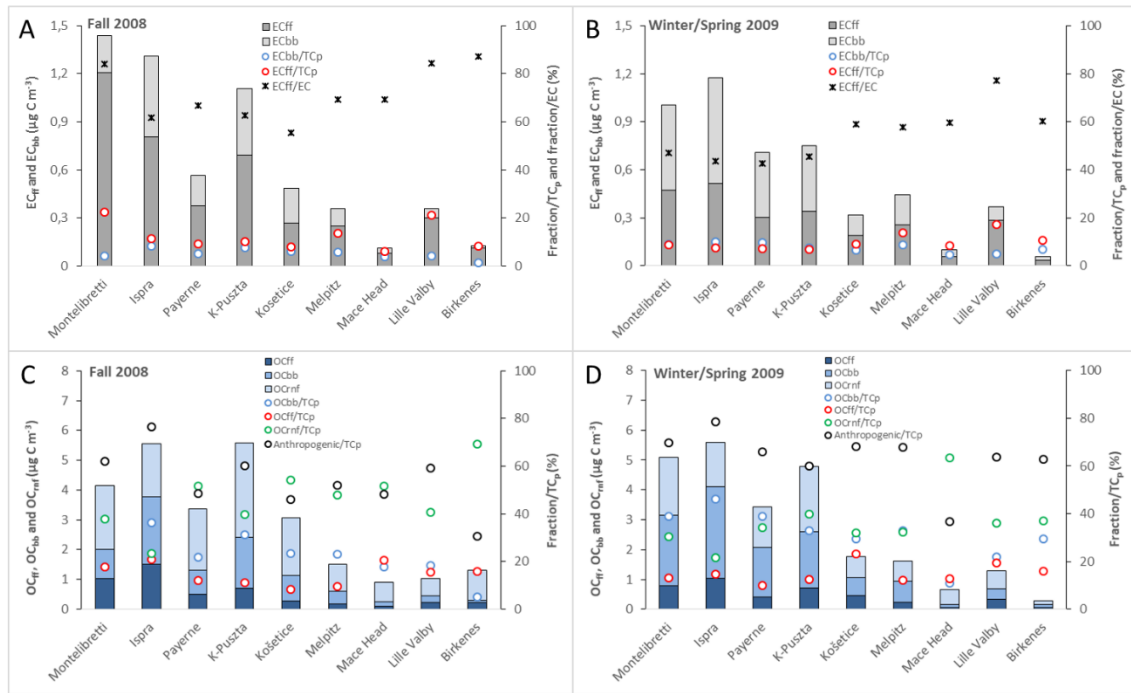


**Figure 2: Mass concentrations of EC from fossil fuel ( $EC_{ff}$ ) and biomass burning ( $EC_{bb}$ ) sources, their fraction of particulate total carbon ( $TC_p$ ) and the fraction of  $EC_{ff}$  to EC for Fall 2008 (panel A) and Winter/Spring 2009 (panel B). Mass concentrations of OC from fossil fuel ( $OC_{ff}$ ), biomass burning ( $OC_{bb}$ ) and remaining non-fossil ( $OC_{nrf}$ ) sources, their fraction of  $TC_p$  and the fraction of Anthropogenic ( $OC_{ff}$ ,  $OC_{bb}$   $EC_{ff}$  and  $EC_{bb}$ ) to  $TC_p$  for Fall 2008 (panel C) and winter/spring 2009 (panel D). The sites are listed by latitude from South to North. Note that the  $EC_{ff}/TC_p$  marker is superimposed on the  $EC_{bb}/TC_p$  marker for Montelibretti and K-Pusztza in panel B, and that the  $OC_{ff}/TC_p$  marker is superimposed on the  $OC_{bb}/TC_p$  marker for Montelibretti in panel C.**

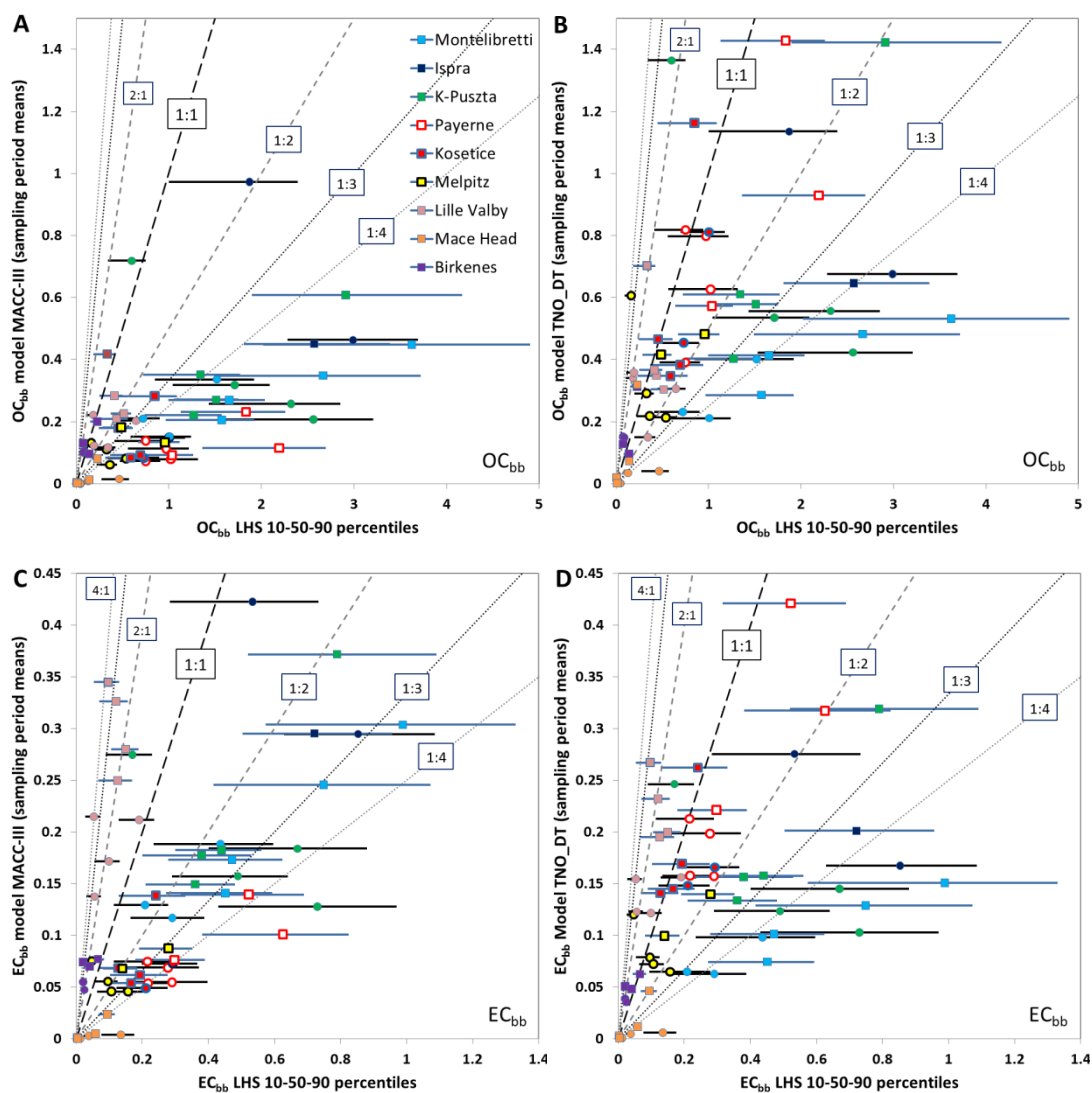


**Figure 3:** Comparison of modelled and measurement/LHS based concentrations of organic and elemental carbon from biomass burning emissions ( $OC_{bb}$  and  $EC_{bb}$ ). The left panels (A and C) show model calculated  $OC_{bb}$  (A) and  $EC_{bb}$  (C) with the base-case model setup, and the right panels (B and D) show the corresponding results using the DT+IVOC model setup. Each point (and horizontal line) represents the results from a single site and week. The lines illustrate the range from the LHS 10-percentile to the 90-percentile and the circles and squares show the LHS-median values. Circles and black horizontal lines show results for Fall 2008 and squares and blue lines show results from Winter/spring 2009. The different sites are identified as follows: Light Blue – Montelibretti; Dark Blue – Ispra; Green – K-puszta; White with red border – Payerne; Red with blue border – Košetice; Yellow with black border – Melpitz; Pink – Lille Valby; Orange – Mace Head; Purple – Birkenes. Unit:  $\mu\text{g C m}^{-3}$ .